To be submitted for publication

LBL-428
Preprint
c. 2

ECM STUDIES OF ENGINEERING MATERIALS IN A FLOW CHANNEL CELL

Daniel Jacquot, Rolf H. Muller and Charles W. Tobias

RECEIVED
LIBRARY

December 1971

DOCUMENTS SECTION

AEC Contract No. W-7405-eng-41

TWO-WEEK LOAN COPY

This is a Library Circulating Copy which may be borrowed for two weeks. For a personal retention copy, call Tech. Info. Division, Ext. 5545

LAWRENCE BERKELEY LABORATORY
UNIVERSITY OF CALIFORNIA

LBL-428
c. 2

25

DISCLAIMER

This document was prepared as an account of work sponsored by the United States Government. While this document is believed to contain correct information, neither the United States Government nor any agency thereof, nor the Regents of the University of California, nor any of their employees, makes any warranty, express or implied, or assumes any legal responsibility for the accuracy, completeness, or usefulness of any information, apparatus, product, or process disclosed, or represents that its use would not infringe privately owned rights. Reference herein to any specific commercial product, process, or service by its trade name, trademark, manufacturer, or otherwise, does not necessarily constitute or imply its endorsement, recommendation, or favoring by the United States Government or any agency thereof, or the Regents of the University of California. The views and opinions of authors expressed herein do not necessarily state or reflect those of the United States Government or any agency thereof or the Regents of the University of California.

ECM STUDIES OF ENGINEERING MATERIALS IN A FLOW CHANNEL CELL

Daniel Jacquot, Rolf H. Muller and Charles W. Tobias

Inorganic Materials Research Division, Lawrence Berkeley Laboratory and Department of Materials Science and Engineering, College of Engineering; University of California, Berkeley, California

ABSTRACT

The anodic dissolution of two heat-resisting alloys, Hastelloy X and Inconel X-750, and of a low carbon steel, SAE 1018, were studied in a channel cell of 0.5 mm gap width under liminar flow conditions in 5N NaCl, $NaClO_3$ and $NaNO_3$ electrolytes. Overall cell voltage and anode and cathode potential measurements were obtained under galvanostatic conditions; in the current density range of 1 to 35 A/cm^2. Micrographs and roughness analysis of the anode surfaces provided additional information. The two alloys demonstrated similar electrochemical behavior regardless of the nature of the electrolyte. However, the choice of anion strongly influenced the anodic dissolution of the low carbon steel. For the latter material, the occurrence of passivation phenomena and anodic oscillations of the potential are related to the formation of anodic films. Models are proposed to explain the dependence of these phenomena on the nature of the electrolyte.

I. INTRODUCTION

Electrochemical Machining (ECM) has found several industrial applications in recent years for the shaping of a variety of metals and alloys. Increasing efforts have been directed toward studying the effects of the various controlling variables involved in this process. ECM studies are most conveniently performed in channel type cells in which electrolyte flows at high velocities (10-10,000 cm/sec) between parallel, closely spaced (0.1-0.5 mm) anode (workpiece) and cathode (tool). The metal is oxidized anodically from the workpiece at current densities in the order of 10 to 150 A/cm^2. The electrode reaction products, which include gases, dissolved and solid matter, are continuously removed by the electrolyte stream.

Most of the recent studies were aimed at clarifying the role of current density, nature of electrolyte and flow rate.[1-7] Efforts have been centered on work with pure metals, involving primarily copper and iron. Evidence related to passivation phenomena, reaction stoicheiometry, steady, as well as oscillatory, anodic potentials observed during dissolution of copper have been reported in the literature.[4,5] The nature of the anion in the electrolyte stream has been shown to strongly influence the anodic dissolution process of copper.[6]

It is of great practical interest to consider the anodic dissolution of certain engineering materials, and to compare their behavior to what has been observed with copper. For this purpose, a study of the anodic behavior of two heat-resisting alloys and a low carbon steel has been undertaken. 5N solutions of sodium chloride, sodium chlorate and sodium nitrate were chosen as electrolytes. The first one is the most widely used electrolyte

in ECM, the second one is well known for its good dimensional control and surface finish, while the last one is commonly used for iron-base and nickel-base alloys.[8]

II. EXPERIMENTAL

Forced convection conditions were obtained with an experimental flow system described earlier.[6] The electrolyte was pumped continuously through the flow channel cell by means of a positive displacement pump. The flow rate was regulated with a needle value in connection with a bypass and then measured with a rotameter. Stainless steel pipes were used throughout the system.

The electrochemical cell employed was one which has been used for the study of the anodic dissolution of copper.[4] The rectangular flow channel had a 0.5 × 8 mm cross section and a 75 mm length, providing defined hydrodynamic conditions at the electrodes. It was made of epoxy resin with an electrode separation of 0.5 mm. Two glass windows allowed optical observation of the electrode gap space (Fig. 1). All the experiments were carried out in laminar flow at a linear flow rate of 50 cm/s. The corresponding Reynolds number was 350 for a 5N NaCl solution.

Both the anode and cathode had a 3.05 × 0.53 mm rectangular shape (area = 1.62 mm^2). A copper cathode was used throughout this study. The anode was made of the studied engineering material cast into epoxy. A stainless steel spacer with a well defined height was used to position the electrode outside the cell. This allowed the electrode surface to be flush with the channel wall. The short dimension of the electrode was oriented parallel to the flow direction to diminish the influence of cathodic gas bubbles on the anodic processes. Two capillaries, drilled into the cell wall, provided for anode and cathode potential measurements.

The constant current power supply* had a maximum output of 3A. The current densities employed ranged from 1 to 35 A/cm^2.

The duration of dissolution runs was so chosen that the anode surface recessed by less than 20 microns; a distance small with respect to the gap dimension. Anode and cathode potentials were measured against saturated calomel electrodes. The steady-state value of the potential was reached after 1 or 2 seconds. The current was recorded by measuring the voltage drop across a precision shunt. Overall cell voltage, electrode potentials and current were recorded simultaneously on a multi channel light beam oscillograph.**

The materials investigated were Hastellogy X, Inconel X-750 and SAE 1018 steel. The latter is a low carbon steel, the two others were heat-resisting Ni-base alloys commonly used for jet engine turbine blades. Their main components are given in Table I. The anodes were fabricated from cold rolled plates followed by a heat treatment procedure, as reported in Table II. An age-hardening process for high temperature service (above 1100°F) was employed for Inconel X-750.[9] The full annealing procedure used for small carbon steel forgings was chosen for SAE 1018.[10] No attempt was made to perform a heat treatment for Hastelloy X.

Ten electrodes were prepared from each material investigated. Thus, a freshly prepared anode was used for each experimental run, involving one value of the current density for a given electrolyte. The electrode preparation consisted of mechanical polishing with 0000 emery paper followed by a metallographic polishing process using a 1μ diamond powder.

---

*Type C618, Electronic Measurements Co. Inc., Eatontown, New Jersey.

**Series 230, Brush Instrument Division, Cleveland, Ohio.

Table I. Main components of the engineering materials investigated (weight %).

	Ni	Cr	Fe	Mo	Ti	C
Hasteolly X	43-52	20-33	17-20	8-10		
Inconel X-750	73	16	7		2.5	
SAE 1018			98-99			0.15-0.20

Table II. Heat treatment used for fabricated anodes.

	Temp., °F	Time (h)	Cooling
Hastelloy X		none	
Inconel X-750	2100	2	air cooled
	1550	24	air cooled
	1300	20	air cooled
SAE 1018	1600	0.5	furnace cooled to 1300°F at 50°F/hour

Because of the hardness of the heat-resisting alloys, in order to obtain a good surface finish, the mechanical polishing was continued for 1 to 2 hours. Following the polishing procedures, the electrode was treated in an ultrasonic cleaner in order to remove any solid particles remaining on the surface after polishing. The electrode was then carefully cleaned with detergent and rinsed with distilled water.

After dissolution in a given electrolyte, micrographs of the anode surface were made, generally when dissolution had occurred at a low and at a high current density value. The magnification used was ×250 for all the photographs. Subsequent Analysis of the profile and the roughness of the anode surface were performed using a skidless surfanalyzer system.* 5N NaCl, $NaClO_3$ and $NaNO_3$ solutions were prepared with technical grade salts and distilled water. All solutions were filtered before using them in the flow channel cell.

*System 150 with drive model 21-1410-01, Clevite Corporation, El Monte, California.

III. RESULTS

5N NaCl Electrolyte

Typical overall cell voltage, anode potential and cathode potential versus time traces for Hastelloy X are shown on Fig. 2. At the beginning of the electrolysis, the cell voltage undergoes irregular low amptitude transients ("fluctuations") of the potential. These fluctuations were more pronounced and lasted longer at higher values of the current density ($i \geqslant 10\ A/cm^2$). The fluctuations were always associated with the cathode potential; the anode potential trace remained flat at all currents. The same typical behavior was observed for Inconel X-750.

Two different dissolution modes appeared in studying SAE 1018. At low current densities, an initial plateau in the cell voltage and anode potential trace was followed by a drop to the steady-state value of the potential (Fig. 3). At higher current densities, an initial anodic peak with fluctuations occurred at the beginning of the dissolution. A steady-state value was subsequently reached with periodic transients ("oscillations") of the potential (Fig. 4). These oscillations were due to the anode potential and their amplitude was approximately 1.3 V. The current density trace (not shown on the figures) remained constant and flat for all the experiments.

In addition to the three materials investigated, copper electrodes were used for parallel experiments. As in the case of SAE 1018, the electrochemical behavior of copper demonstrated two dissolution modes. At low values of the current density, the anode dissolved at a constant low voltage. As the current was increased, a high voltage dissolution mode was reached soon after the current was switched on. This behavior

has been a subject of detailed investigations in this laboratory.[6]

It is of interest to compare the steady-state values of overall cell voltage, anode and cathode potentials against current density, obtained for each material. Figure 5 illustrates the linear voltage vs current density dependence for Hastelloy X which is also typical of the behavior of Inconel X-750. The dashed lines correspond to experiments carried out at a lower flow rate (u = 25 cm/s). For the low carbon steel, both cell voltage and anode potential show a step increase in the potential while the cathode potential increases linearly with current density (Fig. 6). A similar behavior was observed for coper, with a more pronounced jump of potential which occurred at a lower value of the current density.

5N $NaClO_3$ Electrolyte

The anodic behavior of the two heat-resisting allows in chlorate appeared similar to that in chloride medium. No sharp rise of potential was observed over the whole range of current densities investigated. Cathodic fluctuations were still obtained for the highest values of the current density.

The low carbon steel behaved differently that in chloride. For $i \geqslant 10\ A/cm^2$, both cell voltage and anode potential showed regular and well defined oscillations as illustrated in Fig. 7. The amplitude of the anodic oscillations was of the same order of magnitude as the anode potential itself. Fluctuations of the cathode potential were of much smaller amplitude with respect to the average potential. At higher values of the current density, the frequency and the amplitude of the oscillations increased (Fig. 8). An initial peak was formed just before

the beginning of the oscillations. Furthermore, after a certain amount of charge was passed, regular oscillations were followed by irregular ones with a lower amplitude.

Regular anodic oscillations were also observed for copper.* The amplitude was larger while the frequency was of the same order of magnitude as with the low carbon steel. At the highest values of the current density investigated, the periodic phenomena did not last for the whole duration of the electrolysis. After one or two oscillations, the potential jumped to a value representing a high voltage dissolution mode. No more oscillations were observed after the jump of potential. In Fig. 9 the frequency and amplitude of the oscillations are plotted against current density for both copper and SAE 1018.

5N $NaNO_3$ Electrolyte

This electrolyte did not cause significant changes relative to the previously described electrochemical behavior of Hastelloy X and Inconel X-750; the same type of potential-time traces and potential-current density graphs were obtained. Cathodic fluctuations still appeared at high values of the current density.

Small and regular anodic oscillations occurred during the dissolution of SAE 1018 at low current densities (Fig. 10). As the current density was increased, the oscillations became less regular and eventually disappeared just after the beginning of the electrolysis as shown on Fig. 11, an example of the cell voltage undergoing anodic oscillations followed by cathodic fluctuations.

*This typical behavior of copper in chlorate solution is being investigated at present.[11]

Copper dissolved in a low or in a high voltage dissolution mode depending on the current density. Irregular anodic oscillations which decreased in amplitude as the current density was increased occurred in the high voltage mode. The latter phenomenon was comparable to that observed for SAE 1018.

Micrographs and Surface Profile Measurements

Hastelloy X anodes showed the same kind of surface texture for all the electrolytes investigated. Figure 12 is an example of surface texture after dissolution at a high current density value. No drastic change was observed over the range of current density investigated. Surface profile measurements showed the presence of sharp and rounded protrusions over a flat background surface.

Inconel X-750 anode surfaces presented a typical grain boundaries texture independent of the nature of the electrolyte. Figure 13 illustrates grain boundaries and randomly distributed holes. A film layer partially covering the surface could be seen in some micrographs. As for Hastelloy X, the current density did not change the apparent texture of the anode surface.

Unlike for the two alloys, the appearance of low carbon steel surfaces following dissolution depended on current density--and on the nature of the electrolyte. At low current densities, the same surface texture was obtained regardless of the electrolyte used (Fig. 14). The spots have been shown to be holes occurring on a fairly flat surface. At high current densities, the surface texture drastically changed with the nature of the electrolyte as shown on Figs. 15, 16 and 17. In NaCl medium, the surface appears bright with some protrusions and streaks

occurring in the flow direction. In $NaClO_3$ medium, a bright surface was covered almost entirely with a grey film layer. In $NaNO_3$ medium, a complex texture was obtained with film layers partially covering the surface. Examples of surface analysis traces showing holes and protrusions are given in Fig. 19. Surface profiles of representative specimens before anodic dissolution are given in Fig. 18 for comparison.

IV. DISCUSSION

In order to better illustrate the differences and common features of the four materials in, all steady-state values of overall cell voltages are plotted in Figs. 20-22 against current density for each electrolyte used.

For convenience in discussing the whole experimental results, the two heat-resisting alloys will be considered separately from the low carbon steel. The electrochemical behavior of these alloys appears indeed quite similar, while the carbon steel behaves in a complex way and can be better compared to copper.

Heat-Resisting Alloys

Passivation phenomena, oscillations of potential and anodic film layers have been shown to play an important role in ECM. Surprisingly enough, the present investigation revealed neither a jump of potential nor oscillations for the two alloys. The straight lines obtained in the voltage vs current density plots suggest that the same dissolution mode occurred over the range of current densities investigated. The nature of the electrolyte seems to have no significant influence. The complexity of the alloy composition may lead to an overall behavior which obscures the manifestation of characteristics of a particular component. However, the formation of an anodic film cannot be excluded, nor can it be asserted that a passivation phenomenon may not occur at current densities below 1 A/cm^2. Some micrographs showed a film layer partially covering the Inconel X-750 anodes surfaces. Therefore, it is not possible to conclude whether the single dissolution mode observed corresponds to an active (low voltage) or to a transpassive (high voltage) dissolution mode.

Fluctuations of the cell voltage were always due to the cathode potential and are related to the hydrogen evolution. Figure 5 shows that both cell voltage and cathode potential are higher when the flow rate is lower, while the slopes of the straight lines do not change. An increase of the electrolyte resistance close to the cathode surface may be explained by the fact that bubbles tend to grow larger when the flow rate is decreased as suggested by Landolt, et al.[5] who have investigated the nature of cathodic hydrogen revolution under ECM conditions.

The occurrence of protrusions in Hastelloy X surfaces can be related to the presence of a well defined intermetallic compound, randomly distributed in the absence of appropriate heat treatment. The age-hardening pretreatment used for Inconel X-750 leads to recrystallization of the alloy. Metallic precipitates at grain boundaries and selective intergranular attacks have been reported by Kahles.[8] As the composition of the two alloys is fairly comparable, it can be assumed that a heat treatment does influence the surface texture, but has no apparent effect on the electrochemical behavior of the alloy.

Low Carbon Steel and Copper

The anodic dissolution of copper and iron in various electrolytes under broad current density and flow conditions has received relatively close attention in the past. It is usually accepted now that passivation is related to the formation of anodic films. The influence of the anion of the electrolyte on the formation and removal of these films is, at present, the subject of intensive investigations. Chlorate solution has been found to be especially suitable with respect to dimensional accuracy and surface finish. More information can, therefore, be

drawn from the literature about the dissolution of metals in chlorate than in chloride or nitrate. For the sake of convenience, the results obtained in the present work in 5N $NaClO_3$ solution will be discussed first.

Chlorate Solution

By reflection electron diffraction studies, Hoare and his co-workers[1] have shown evidence of films of γ-Fe_2O_3 on soft iron electromachined in $NaClO_3$ solution. Furthermore, they detected high percentage of oxygen on the anode surface following disolution in chlorate. In studying the passivation of iron in borate-boric acid solution, Nagayama and Cohen[12] suggested that the inner layer of the oxide film is composed of Fe_3O_4. It is assumed that a protective and porous film of γ-Fe_2O_3 or Fe_3O_4 or a mixture of the two,[2] is formed on the surface and is responsible for the passivation of iron in chlorate medium.

Taking into account the anodic ascillations shown in Fig. 7, the following model is proposed. At the lowest current densities, the system is active and iron is dissolved as Fe^{++} ions which can undergo further oxidation.[1] As the current is increased, the surface becomes passivated by the formation of a film of γ-Fe_2O_3 and consequently the potential increases abruptly. The oxide film can be formed by oxidation of either Fe or Fe^{++} [13] according to

$$2\ Fe + 3\ H_2O \longrightarrow Fe_2O_3 + 6\ H + 6\ e \qquad (1)$$

$$2\ Fe^{++} + 3\ H_2O \longrightarrow Fe_2O_3 + 6\ H^+ + 2\ e \qquad (2)$$

Chin[3] reported that the rate of γ-Fe_2O_3 film growth increases with the increase in the rate of iron dissolution. This leads first to assume that reaction (2) would occur rather than reaction (1). Furthermore, this information allows one to explain why the frequency of the oscillations increases (as shown in Fig. 9) when the current density, and therefore the rate of iron dissolution, increases.

The iron dissolution is inhibited by the film formation process due to the spreading of the oxide, which reduces the area of active sites where the dissolution occurs.[3] Since the film is supposed to be porous, the dissolution of iron to Fe^{++} ions is still possible, though inhibited. An important part of the current is consumed by oxygen evolution, instead of by iron dissolution, according to

$$2\ H_2O \longrightarrow O_2 + 4\ H^+ + 4\ e$$

The film removal could be caused by oxygen bubbles which are generated between the metal and the porous oxide. A mechanical effect would, therefore, cause the removal of the layer.

At higher currents, a first initial peak is observed before the beginning of the oscillations (Fig. 8). It is likely that a film of Fe_3O_4 is formed by oxidition of either Fe or Fe^{++}, which is further xoidized to γ-Fe_2O_3. It is not understood why this initial step occurs before the periodic film formation and removal. As the current is increased, the frequency of the oscillations increases, as previously explained. After a certain amount of charge is passed, regular oscillations are followed by irregular ones with a low amplitude. Increasing amounts of Cl^- and decreasing ClO_3^- ion concentration were measured for

extented periods of electrolysis.[1] The following reaction needs to be considered

$$6\ Fe^{++} + NaClO_3 + 3\ H_2O \longrightarrow 6\ Fe^{+++} + NaCl + 6\ OH^-$$

According to Hoar,[14] the chloride ion can penetrate and dissolve films of iron oxides so that the surface is not passivated by a protective oxide film. According to this model, the formation γ-Fe_2O_3 is inhibited by the Cl^- ion and the film is removed before spreading over the surface. Thus, dissolution of iron as Fe^{++} ions should play a critical role in the dissolution process. This is in good agreement with the fact that the average of the irregular oscillations corresponds to the initial value of the potential.

One might think that the influence of the chloride ion could be more important than the oxygen bubbles in the periodic removal of the γ-$F3_2O_3$ film. The model described takes into account that for ECM in chlorates, oxygen liberation at significant rates has been reported. On the other hand, except for extended periods of electrolysis, only small concentrations of chloride ions have been detected. Clearly, further investigations are needed to support or demolish either of these assumptions.

Chloride Solution

Hoare and his co-workers,[1] detected neither a film of γ-Fe_2O_3 nor the presence of oxygen on iron specimens electro-machined in NaCl solution. No passivation phenomena were assumed to occur in chloride medium. In a later paper, Hoare[2] reported the formation of a porous, nonprotective film on iron in chloride solution, which is removed at

high anodic potentials. More recently, Chin[3] showed evidence of passivation of a steel anode in NaCl electrolyte. The passivation was attributed to the formation of an adsorbed layer of anodic products. Ferrous compounds, such as $Fe(OH)_2$, were assumed to precipitate on the anode surface forming a porous, nonprotective film. In studying the dissolution of copper in NaCl solution, Kinoshita[6] suggested that a layer of CuCl was formed due to the stability of the monovalent ionic state.

Although the presence of anodic films in chloride medium has been reported in the literature,[3] no evidence seems to have been obtained about their composition. It is suggested that, in the case of iron as well as in that of copper, usually unstable ionic states become thermodynamically more favorable than the stable ionic states. At the end of the electrolysis, the film could decompose or dissolve as soon as the current is switched off. As reported by Chin,[3] since the film is very porous, it can be washed away easily with a jet of water. Any attempt to further identify the anodic film products would therefore be difficult.

The overall cell voltage-current density graph shown in Fig. 20 indicates the occurrence of a passivation phenomenon on low carbon steel. The following sequence may be suggested: metal dissolves first as Fe^{++} ions leading to further precipitation of ferrous compounds on the anode surface. By analogy with copper, it is suggested that a thin and porous layer of $FeCl_2$ is formed which allows the iron dissolution to continue through the pores. At high current densities, small oscillations take place as shown in Fig. 4. The possibility of formation and removal of

ferrous hydroxyde layers cannot be discounted, either. More detailed investigations are needed on this question. It is nevertheless possible to start from a porous and nonprotective film model of ferrous compounds, even if the presence of such a film cannot be proven on the basis of the present investigation. The occurrence of a bright surface with randomly distributed protrusions (Fig. 15) suggests that iron was dissolved in a transpassive dissolution mode.

Nitrate Solution

Little information is available about the nature of anodic films in the dissolution of metals in nitrate medium. In studying the dissolution of copper in 2N KNO_3 solution, Kinoshita, et al.[6] detected the presence of Cu_2O as the main constituent of solid anodic products. The onset of passivation was shown to coincide with the limiting transport of dissolved reaction products by convective diffusion. Landolt, et al.[4] reported that passivation of copper anodes occurred with the formation of a thick layer which seemed to disappear just after the current was switched off.

Figure 22 shows a typical graph for the dissolution of copper. The overall cell voltage-current density graph for the low carbon steel is represented by a straight line. This suggests a unique dissolution mode, iron dissolving mainly as Fe^{++} ions. As for the two heat-resisting alloys, it cannot be concluded that dissolution occurs in an active mode. Both figures 10 and 11 show anodic oscillations of low amplitude. It is assumed that small amounts of γ-Fe_2O_3 are formed and removed according to the model previously described. Film layers partially covering the

surface can be seen in Fig. 17. Figure 16 shows the presence of larger granules of solid anodic reaction products in chlorate solution, than in nitrate. Possibly in nitrate medium, the oxide film doesn't spread all over the surface but is restricted to some active sites before being removed. This leads to the assumption that oxygen evolution is more important in nitrate than in chlorate solution. Oxygen analysis and current efficiency measurements would be of interest to bring about a more detailed understanding of the basic phenomena observed throughout this work.

V. SUMMARY AND CONCLUSIONS

The present work was aimed at investigating the gross electrochemical behavior of engineering materials in various electrolytes commonly used in the technical ECM process. Additional information was drawn from micrographs and surface profiles of the materials.

Overall cell voltage and anode potential versus current density graphs show that the two heat resisting alloys dissolve in the same dissolution mode over the range of current densities investigated. Neither an abrupt jump of potential nor anodic oscillations were observed in chlorate, chloride and nitrate solutions. Although the nature of the electrolyte is well known to play an important role in ECM, the anion types employed had no apparent influence on the electrochemical behavior of these alloys. Heat treatment does influence the surface texture and leads to a grain boundary texture with intergranual attack. Evidence was obtained on fluctuations of the potential at high current densities caused by cathodic gas evolution.

On the other hand, the behavior of the low carbon steel shows a strong dependence on the electrolyte anion. Passivation phenomena and anodic oscillations were observed, for the steel as well as for copper, and are related to the formation of anodic film layers. In $NaClO_3$ solutions, a model is proposed to obtain a better understanding of the relationship between regular oscillations and anodic film formation and removal. In this medium, the film is assumed to be an oxide composed mainly of γ-Fe_2O_3. Two different dissolution modes were observed in chloride solutions. Here, passivation is attributed to the formation

of a layer of adsorbed anodic products. Ferrous compounds are assumed to precipitate on the iron surface as a thin and porous layer. In nitrate solutions, potential-current density graphs indicate a single dissolution mode. This suggests that the main anodic reaction is iron dissolution as ferrous ions. Anodic oscillations with a low amplitude were observed in nitrate as well as in chloride electrolytes; their amplitude was comparable to the average potential in chlorate solutions. It is probably that these phenomena play a significant role in the practical electromachining process of iron and copper and the excellent ECM properties of the chlorate solution for these materials may be related to anodic oscillation phenomena.

REFERENCES

1. J. P. Hoare, M. A. LaBoda, M. L. McMillan and A. T. Wallace, Jr., J. Electrochem. Soc., 116, 199 (1969).
2. J. P. Hoare, ibid, 117, 142 (1970).
3. D. T. Chin, ibid, 118, 174 (1971).
4. D. Landolt, R. H. Muller and C. W. Tobias, ibid, 117, 1246 (1970).
5. D. Landolt, R. Acosta, R. H. Muller and C. W. Tobias, ibid, 117, 839 (1970).
6. K. Kinoshita, D. Landolt, R. H. Muller, and C. W. Tobias, ibid, 117, 1246 (1970).
7. A. E. Debazz and D. A. Olivez, Electrochemical Machining, (American Elsevier, New York, 1968).
8. J. F. Kahles, Metals Handbook, 8th ed., 3, 233 (1961).
9. Engineering Properties of Inconel Alloy X-750, (Technical Bulletin T-38), Huntington Alloy Products Division, The International Nickel Company, Inc., p. 9.
10. Metals Handbook, 8th ed., American Society for Metals, 2, p. 3.
11. J. Cooper, to be published.
12. M. Nagayama and M. Cohen, J. Electrochem. Soc., 109, 781 (1962).
13. M. Pourbaix, Atlas of Electrochemical Equilibria in Aqueous Solutions, (Brussels, 1st ed., 307-321, 1966).
14. T. P. Hoar, Corrosion Sci., 7, 341 (1967).

FIGURE CAPTIONS

Fig. 1 Photograph of the electrochemical flow cell.

Fig. 2 Oscillograph traces for Hastelloy X dissolution in 5N NaCl at 20 A/cm^2.

Fig. 3 Oscillograph traces for SAE 1018 dissolution in 5N NaCl at 2 A/cm^2.

Fig. 4 Oscillograph traces for SAE 1018 dissolution in 5N NaCl at 15 A/cm^2.

Fig. 5 Measured potentials during Hastelloy X dissolution in 5N NaCl at two flow rates—u = 50 cm/s,--u = 25 cm/s.

Fig. 6 Measured potentials during SAE 1018 dissolution in 5N NaCl, u = 50 cm/s.

Fig. 7 Oscillograph traces for SAE 1018 dissolution in 5N $NaClO_3$ at 10 A/cm^2.

Fig. 8 Oscillograph traces for SAE 1018 dissolution in 5N $NaClO_3$ at 35 A/cm^2.

Fig. 9 Measured amplitudes and frequencies of cell voltage oscillations during anodic dissolution of copper and SAE 1018 in 5N $NaClO_3$, u = 50 cm/s.

Fig. 10 Oscillographs traces for SAE 1018 dissolution in 5N $NaNO_3$ at 10 A/cm^2.

Fig. 11 Oscillographs traces for SAE 1018 dissolution in 5N $NaNO_3$ at 25 A/cm^2.

Fig. 12 Micrograph of Hastelloy X surface after dissolution in 5N $NaClO_3$ at 30 A/cm^2.

Fig. 13 Micrograph of Inconel X-750 after dissolution in 5N $NaClO_3$ at 30 A/cm^2.

Fig. 14 Micrograph of SAE 1018 after dissolution in 5N $NaClO_3$ at 5 A/cm^2.

Fig. 15 Micrograph of SAE 1018 after dissolution in 5N NaCl at 20 A/cm^2.

Fig. 16 Micrograph of SAE 1018 after dissolution in 5N $NaClO_3$ at 15 A/cm^2.

Fig. 17 Micrograph of SAE 1018 after dissolution in 5N $NaNO_3$ at 30 A/cm^2.

Fig. 18 Surface profile measurements before anodic dissolution. a) SAE 1018 b) Hastelloy X.

Fig. 19 Surface profile measurements after anodic dissolution. a) SAE 1018 in 5N $NaClO_3$ at 5 A/cm^2 b) Hastelloy X in 5N NaCl at 20 A/cm^2.

Fig. 20 Measured cell voltages for the anodic dissolution of copper, SAE 1018, Hastelloy X and Inconel X-750 in 5N NaCl. The IR drop was calculated on the basis of a molar conductance for 5N NaCl of 50 Ω^{-1} cm^2 $mole^{-1}$ (from Chapman-Newman). Flow velocity 50 cm/sec.

Fig. 21 Measured cell voltages for the anodic dissolution of copper, SAE 1018, Hastelloy X, and Inconel X-750 in 5N $NaClO_3$. Flow velocity 50 cm/sec amplitude of the oscillations for SAE 1018. amplitude of the oscillations for copper.

Fig. 22 Measured cell voltages for the anodic dissolution of copper, SAE 1018, Hastelloy X and Inconel X-750 in 5N $NaNO_3$. Flow velosity 50 cm/sec.

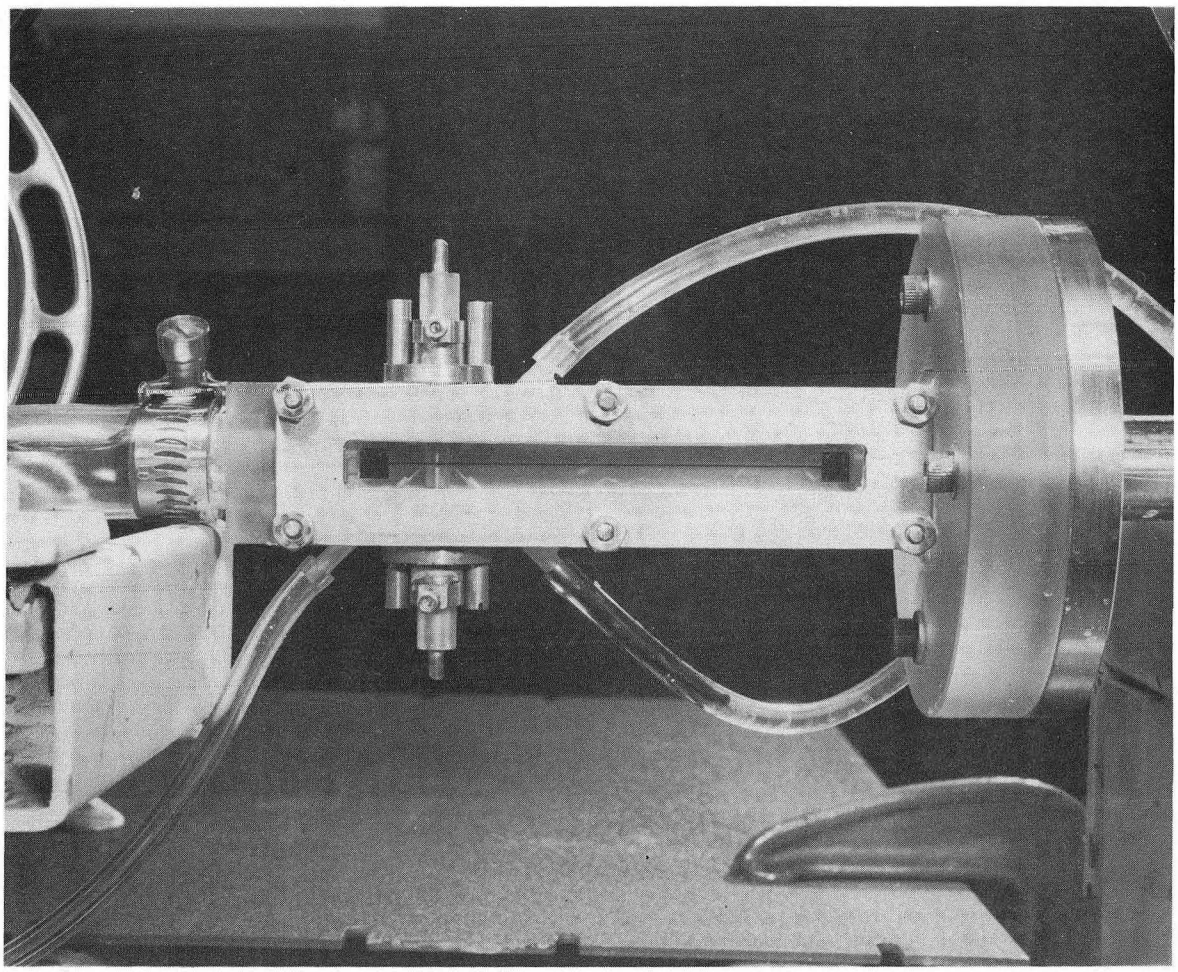

CBB 6712-7051

Fig. 1

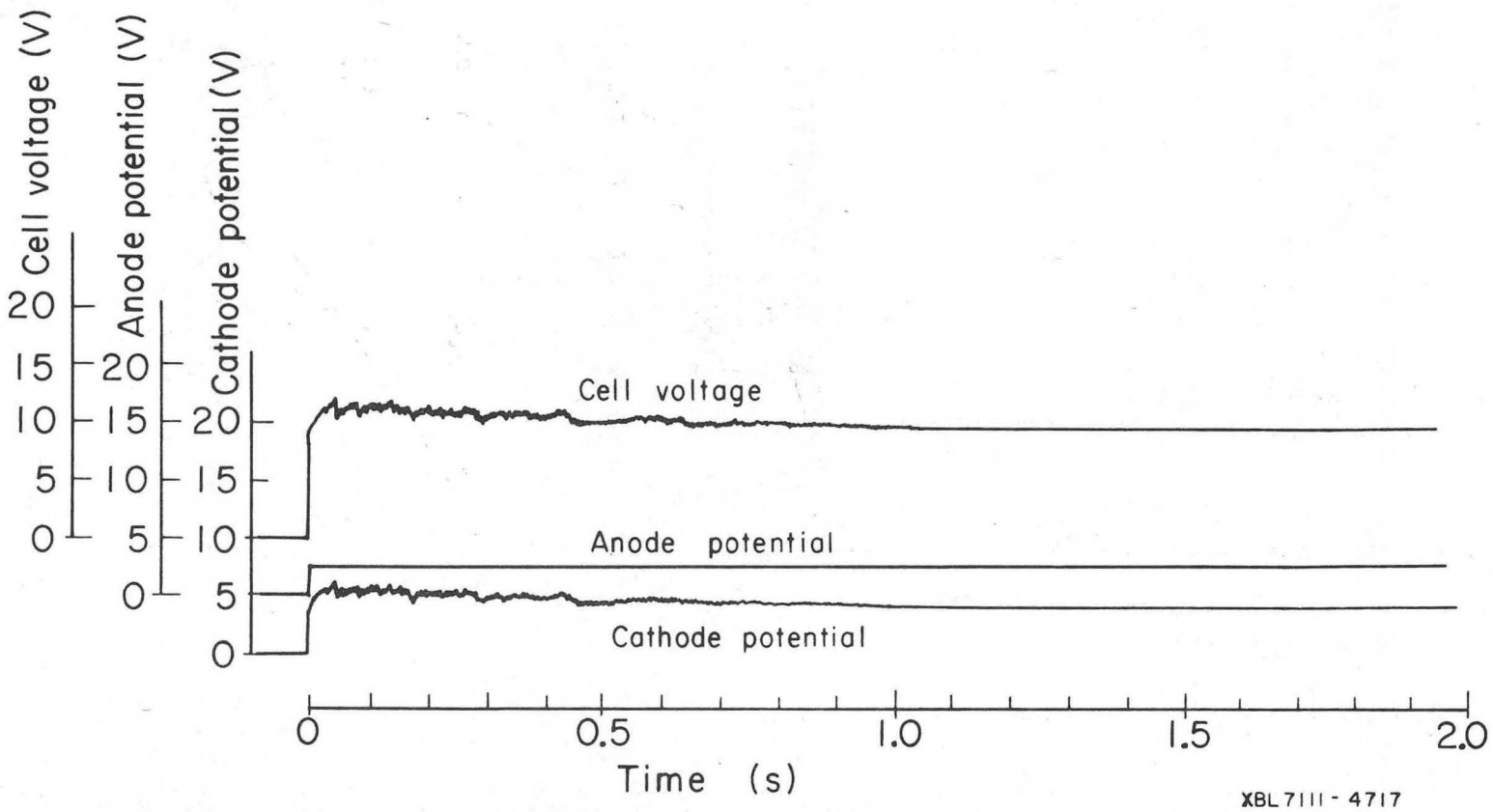
Cell voltage (V)
Anode potential (V)
Cathode potential (V)
20
15
10
5
0
20
15
10
5
0
20
15
10
5
0
Cell voltage
Anode potential
Cathode potential
0
0.5
1.0
1.5
2.0
Time (s)
XBL 7111 - 4717

Fig. 2

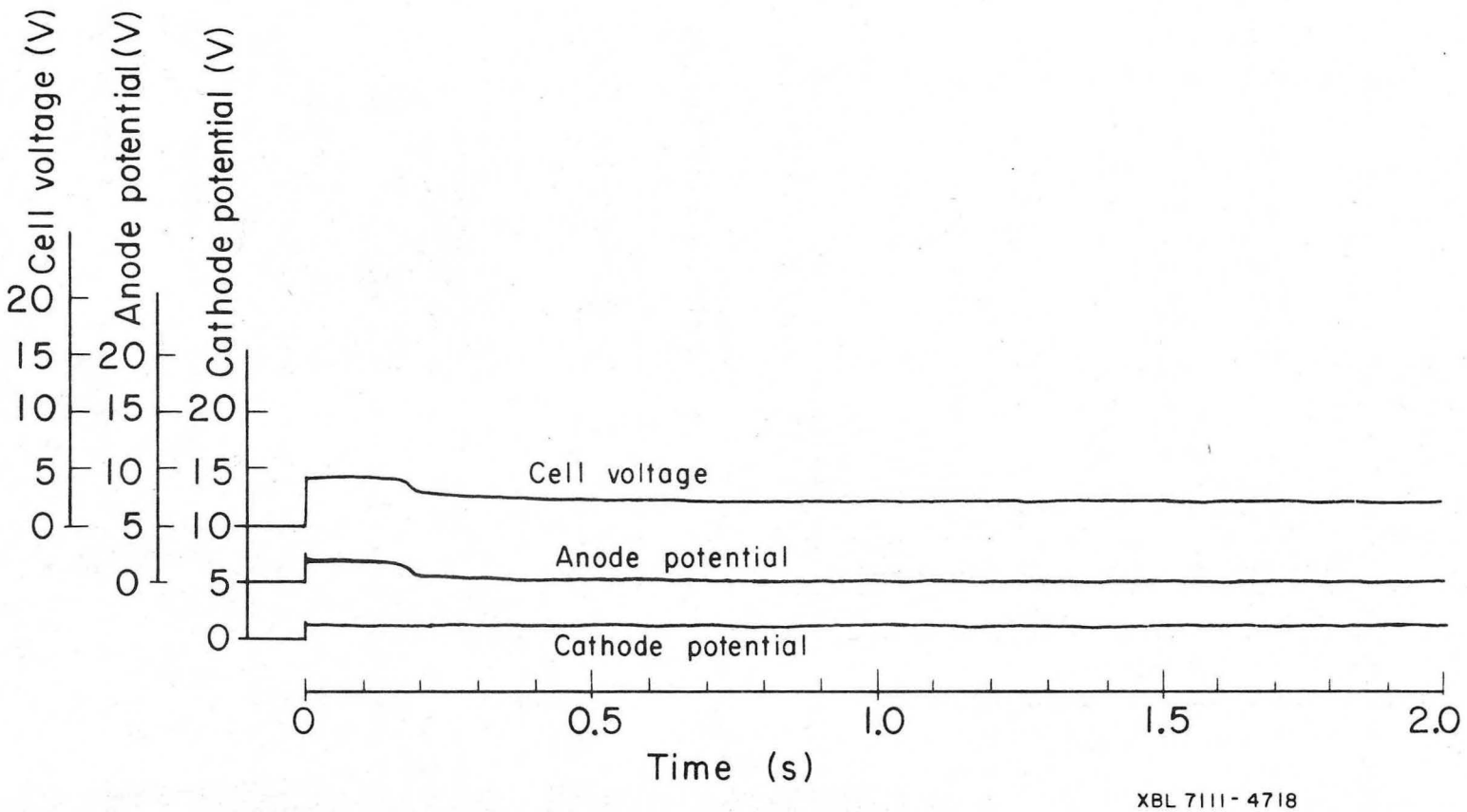
Cell voltage (V)
Anode potential (V)
Cathode potential (V)
20
15
10
5
0
20
15
10
5
0
20
15
10
5
0
Cell voltage
Anode potential
Cathode potential
0
0.5
1.0
1.5
2.0
Time (s)
XBL 7111-4718

Fig. 3

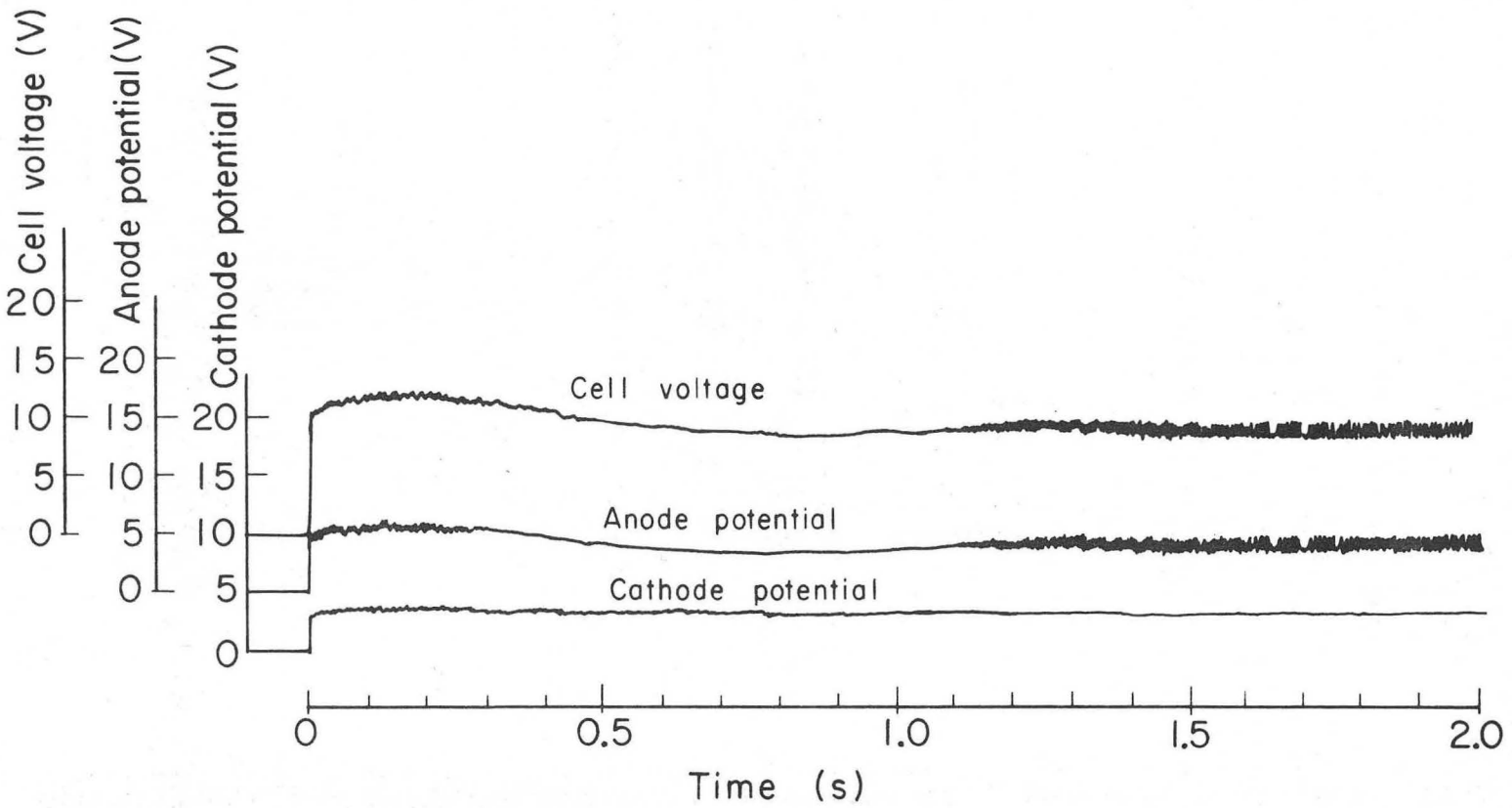

XBL7111-4716

Fig. 4

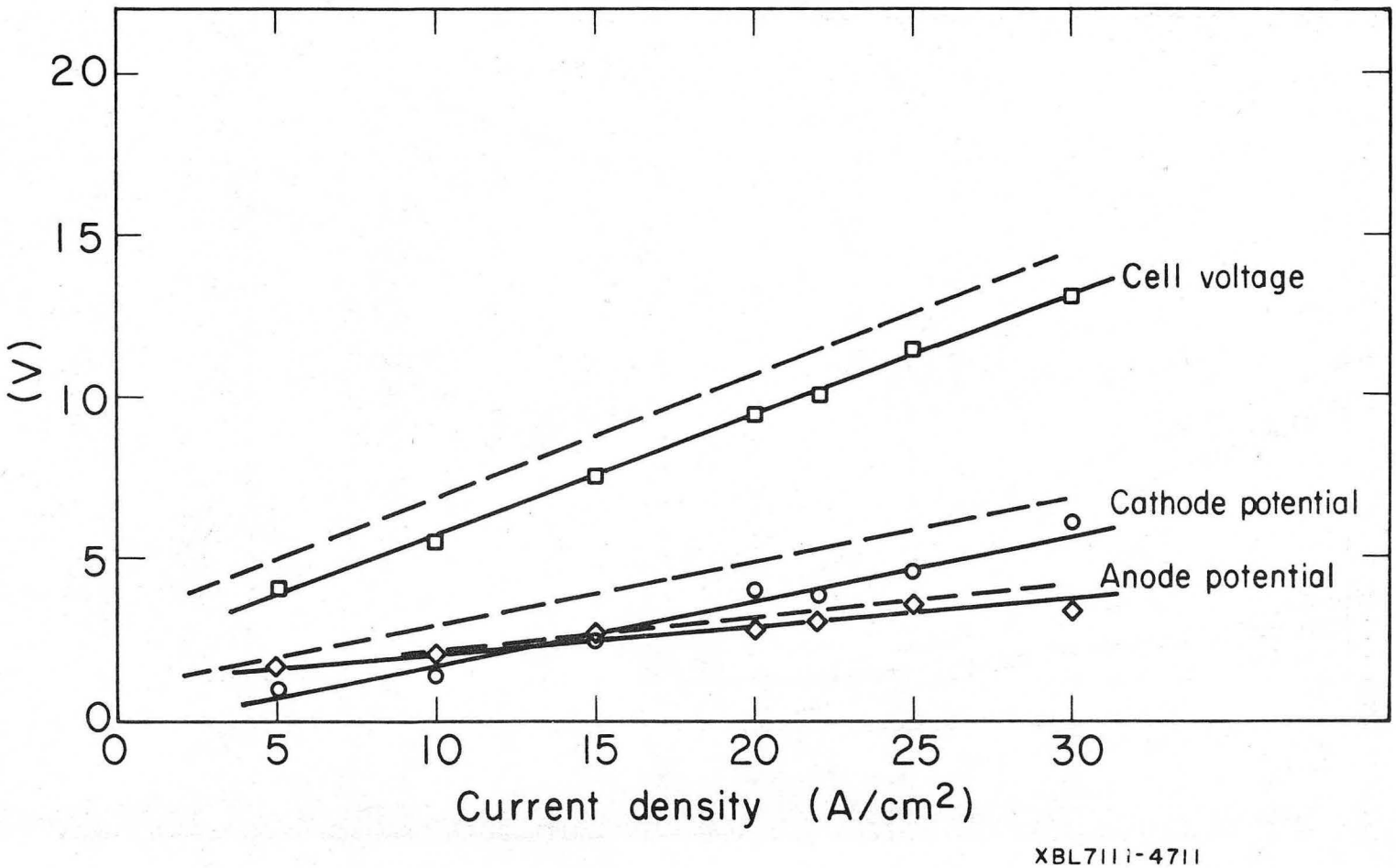
20
15
10
5
0
(V)
0
5
10
15
20
25
30
Current density (A/cm2)
Cell voltage
Cathode potential
Anode potential
XBL7111-4711

Fig. 5

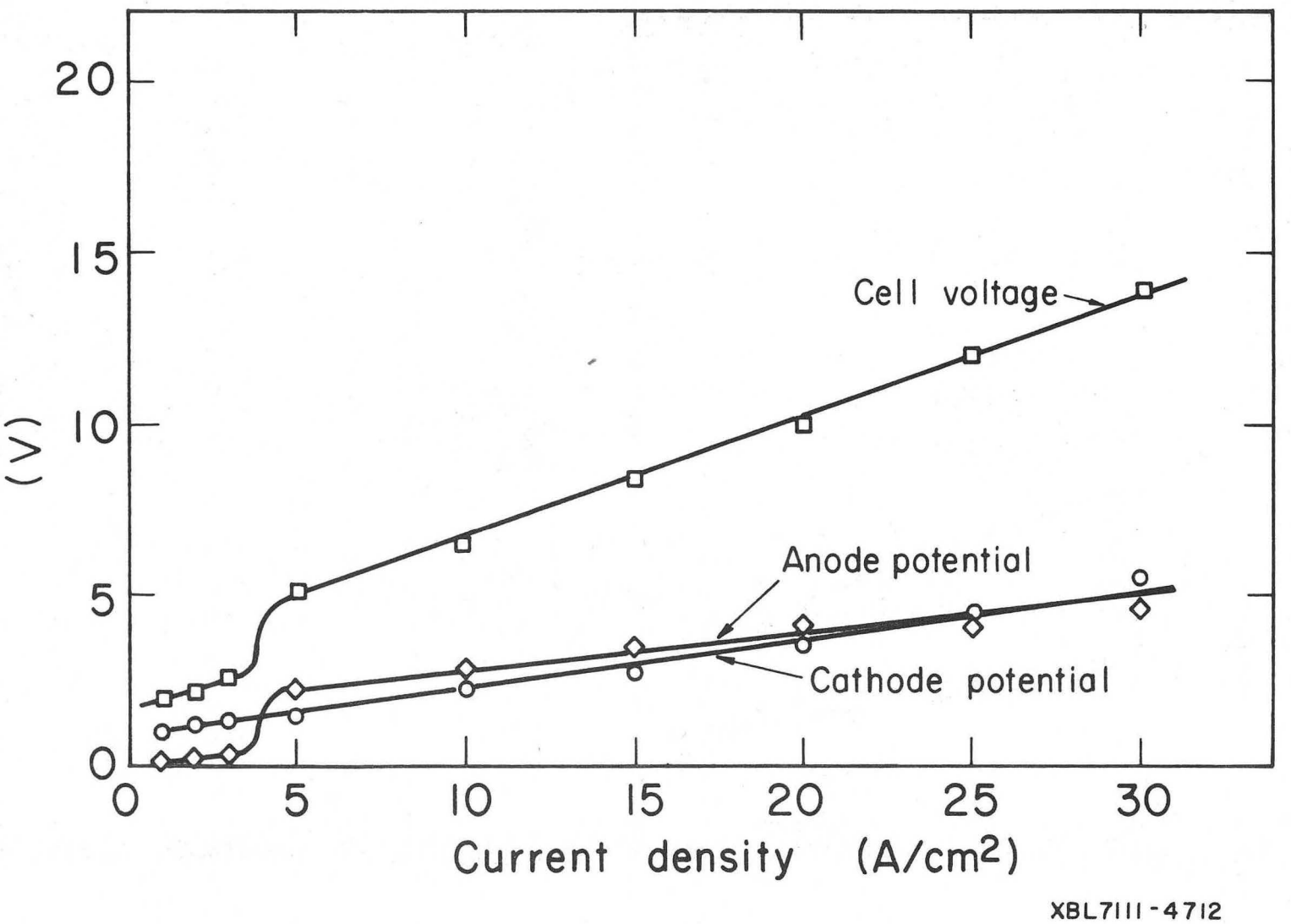
20
15
10
5
0
(V)
Cell voltage
Anode potential
Cathode potential
0
5
10
15
20
25
30
Current density (A/cm2)
XBL7111-4712

Fig. 6

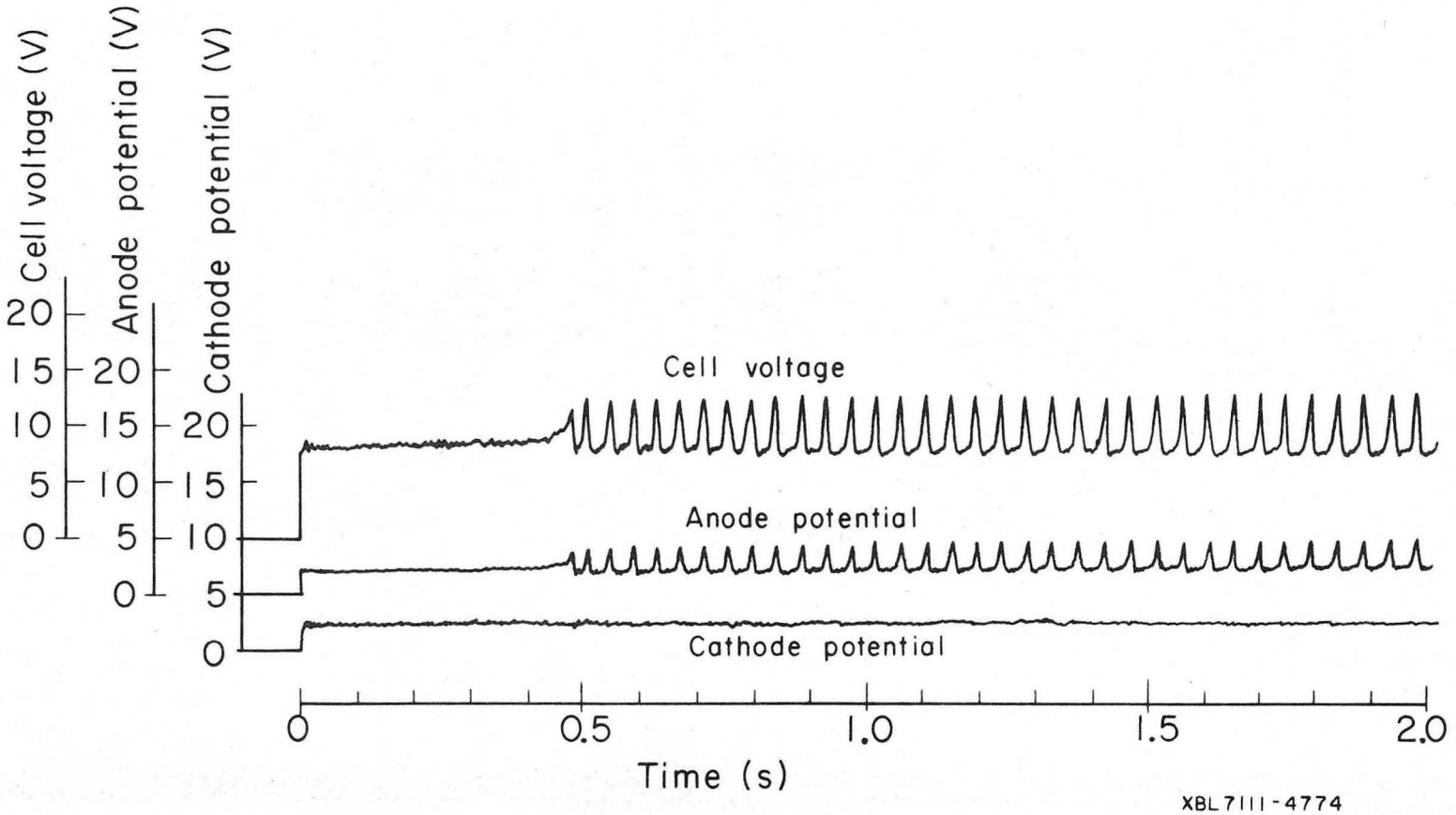
Cell voltage (V)
Anode potential (V)
Cathode potential (V)
20
15
10
5
0
20
15
10
5
0
20
15
10
5
0
Cell voltage
Anode potential
Cathode potential
0
0.5
1.0
1.5
2.0
Time (s)
XBL 7111-4774

Fig. 7

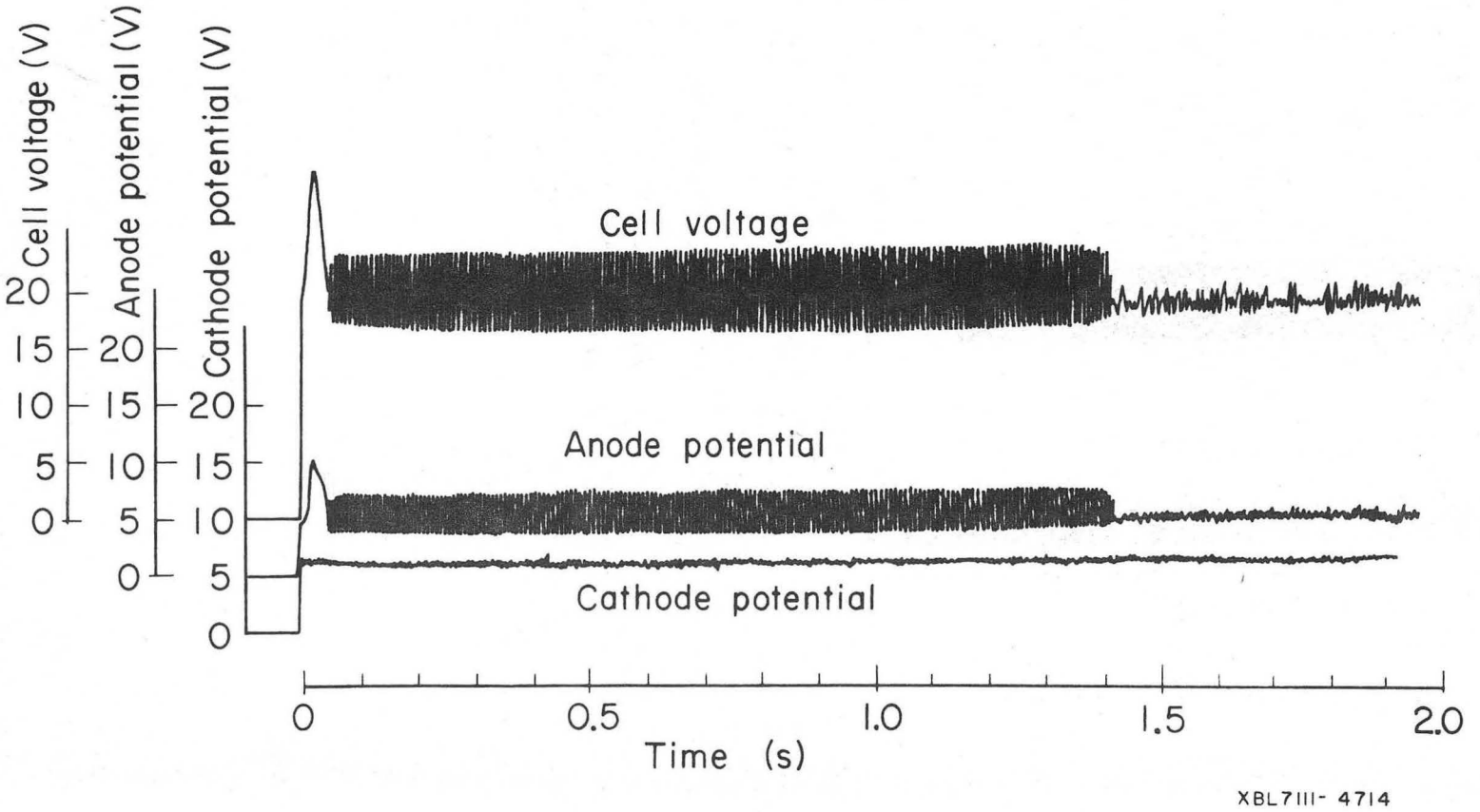
Cell voltage (V)
Anode potential (V)
Cathode potential (V)
20
15
10
5
0
20
15
10
5
0
20
15
10
5
0
Cell voltage
Anode potential
Cathode potential
0
0.5
1.0
1.5
2.0
Time (s)
XBL7111-4714

Fig. 8

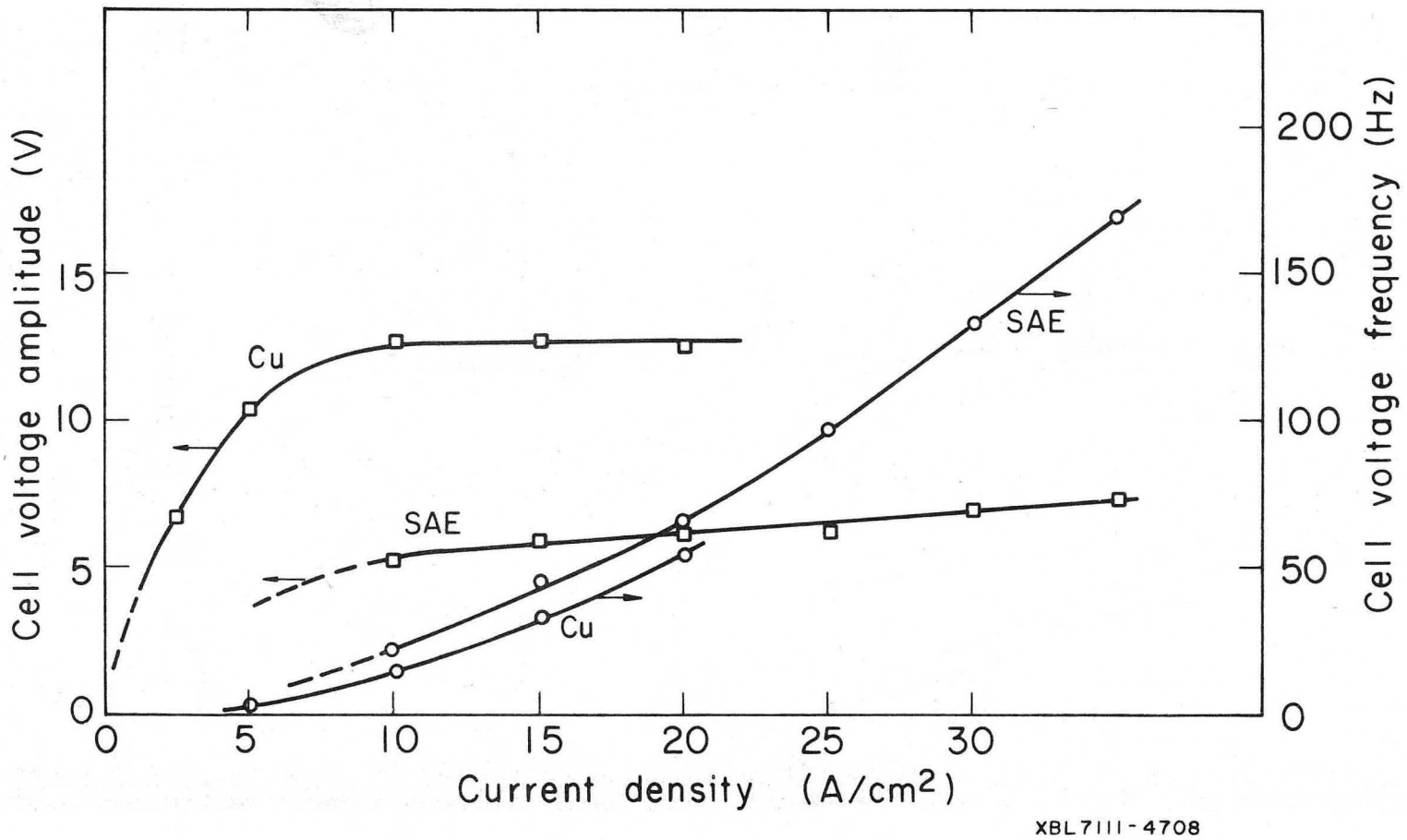
Cell voltage amplitude (V)
Cell voltage frequency (Hz)
Current density (A/cm2)
0
5
10
15
20
25
30
50
100
150
200
Cu
SAE
SAE
Cu
XBL7111-4708

Fig. 9

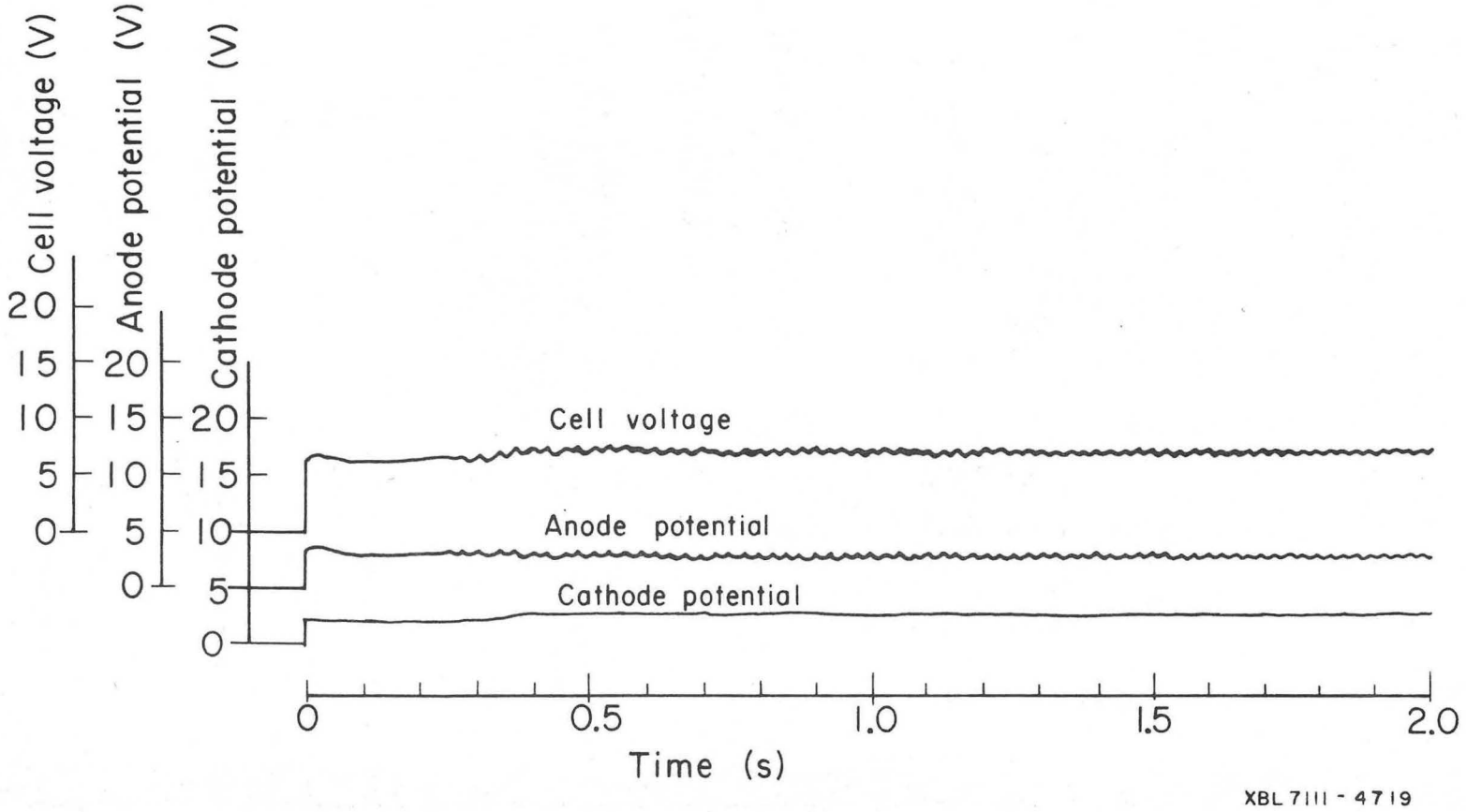
Cell voltage (V)
Anode potential (V)
Cathode potential (V)
20
15
10
5
0
20
15
10
5
0
20
15
10
5
0
Cell voltage
Anode potential
Cathode potential
0
0.5
1.0
1.5
2.0
Time (s)
XBL 7111 - 4719

Fig. 10

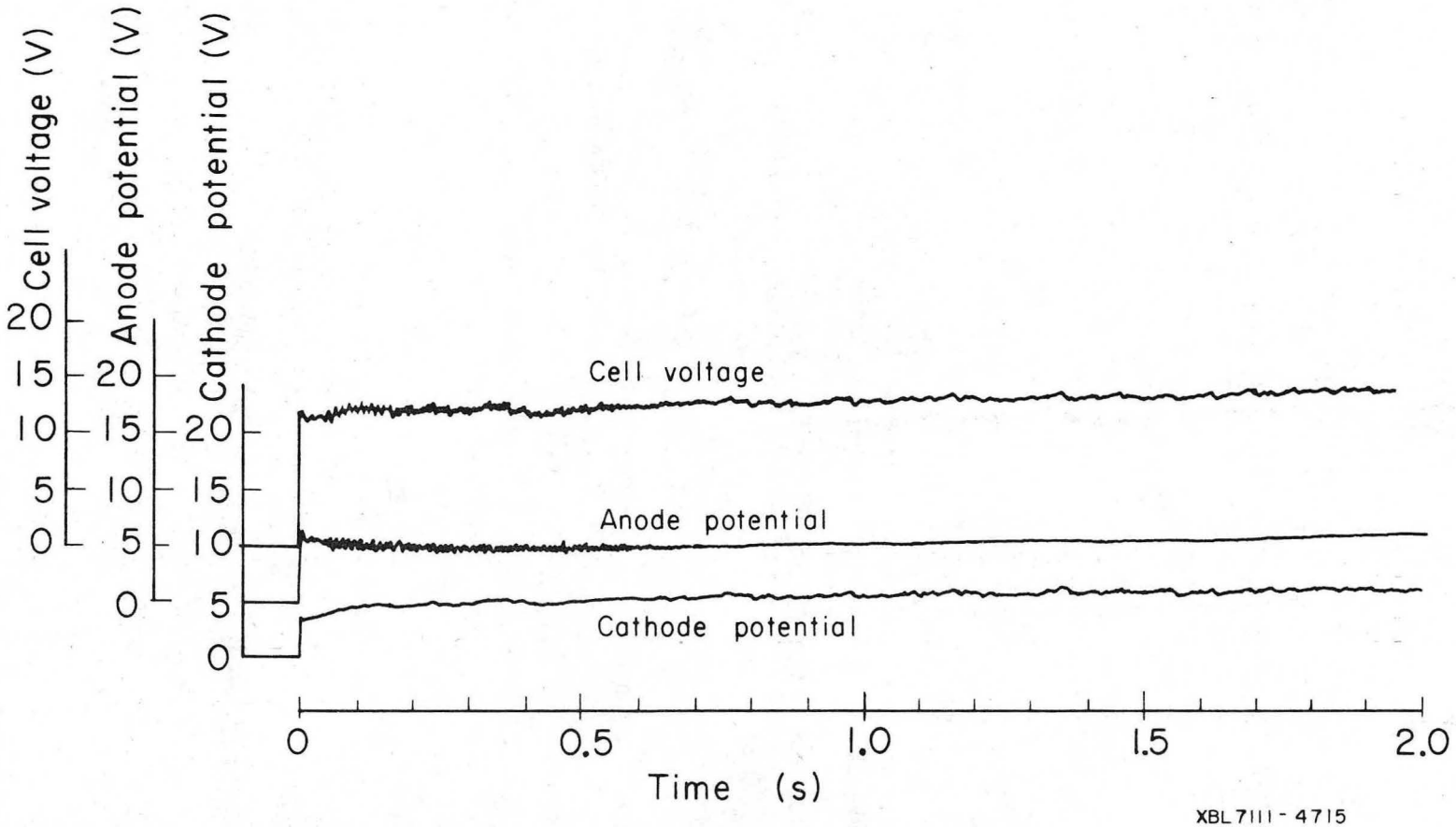
Cell voltage (V)
Anode potential (V)
Cathode potential (V)
20
15
10
5
0
20
15
10
5
0
20
15
10
5
0
Cell voltage
Anode potential
Cathode potential
0
0.5
1.0
1.5
2.0
Time (s)
XBL 7111-4715

Fig. 11

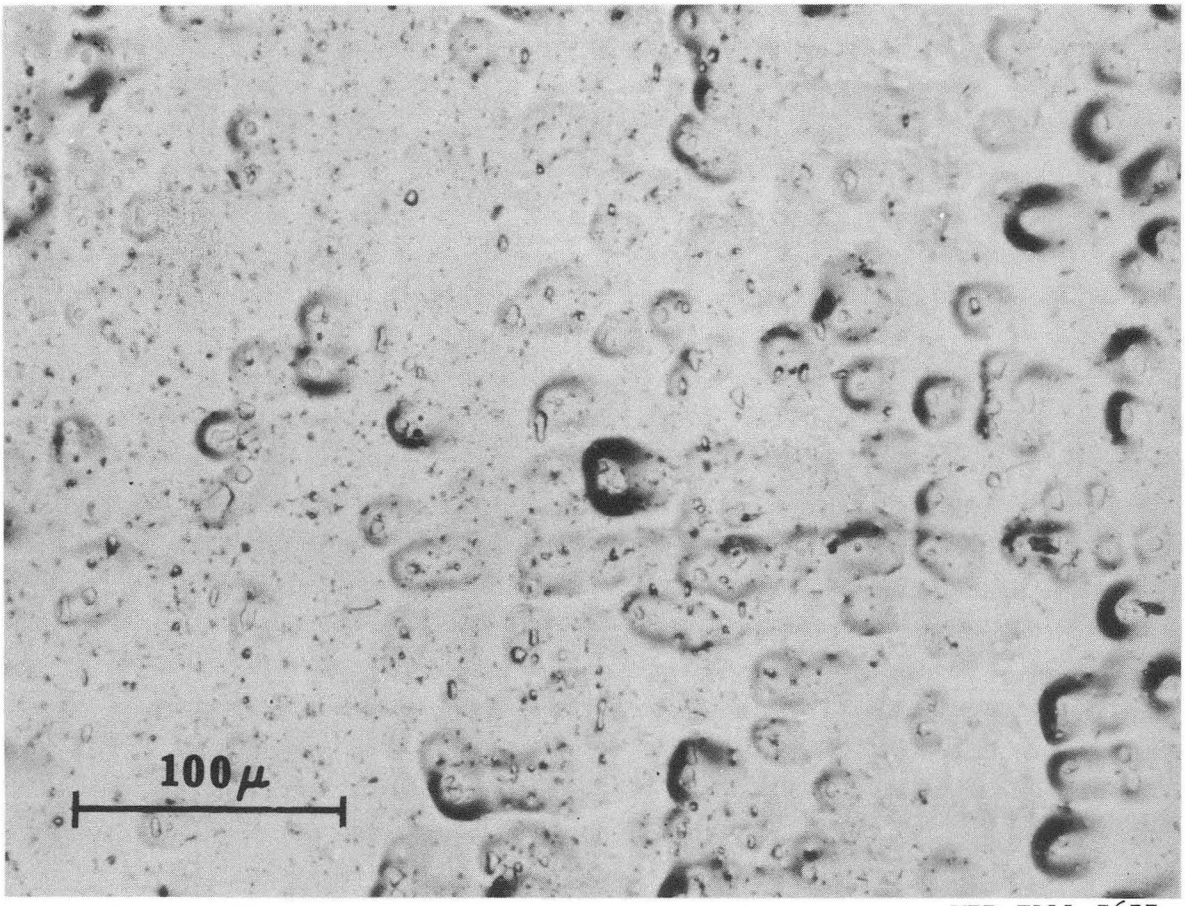

XBB 7111-5655

Fig. 12

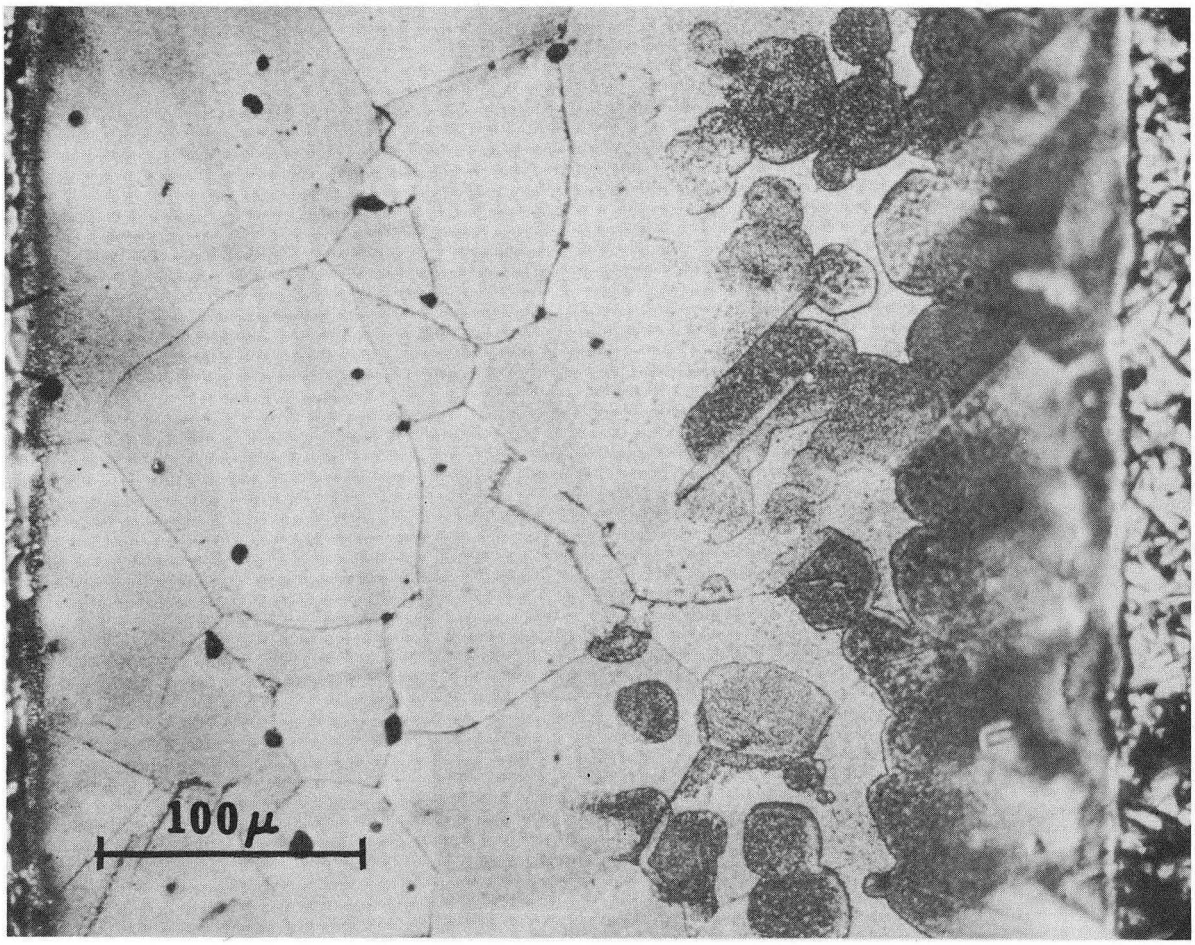

XBB 7111-5657

Fig. 13

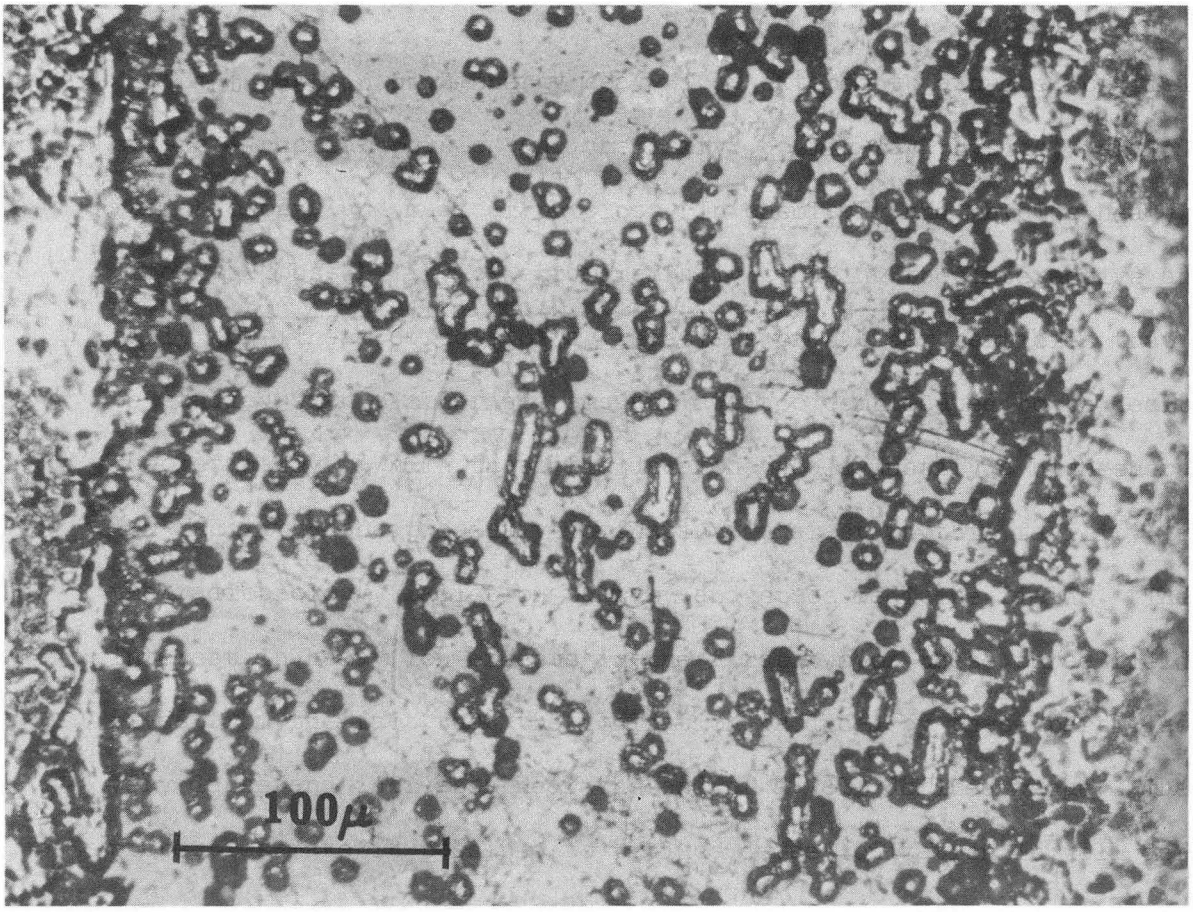

XBB 7111-5652

Fig. 14

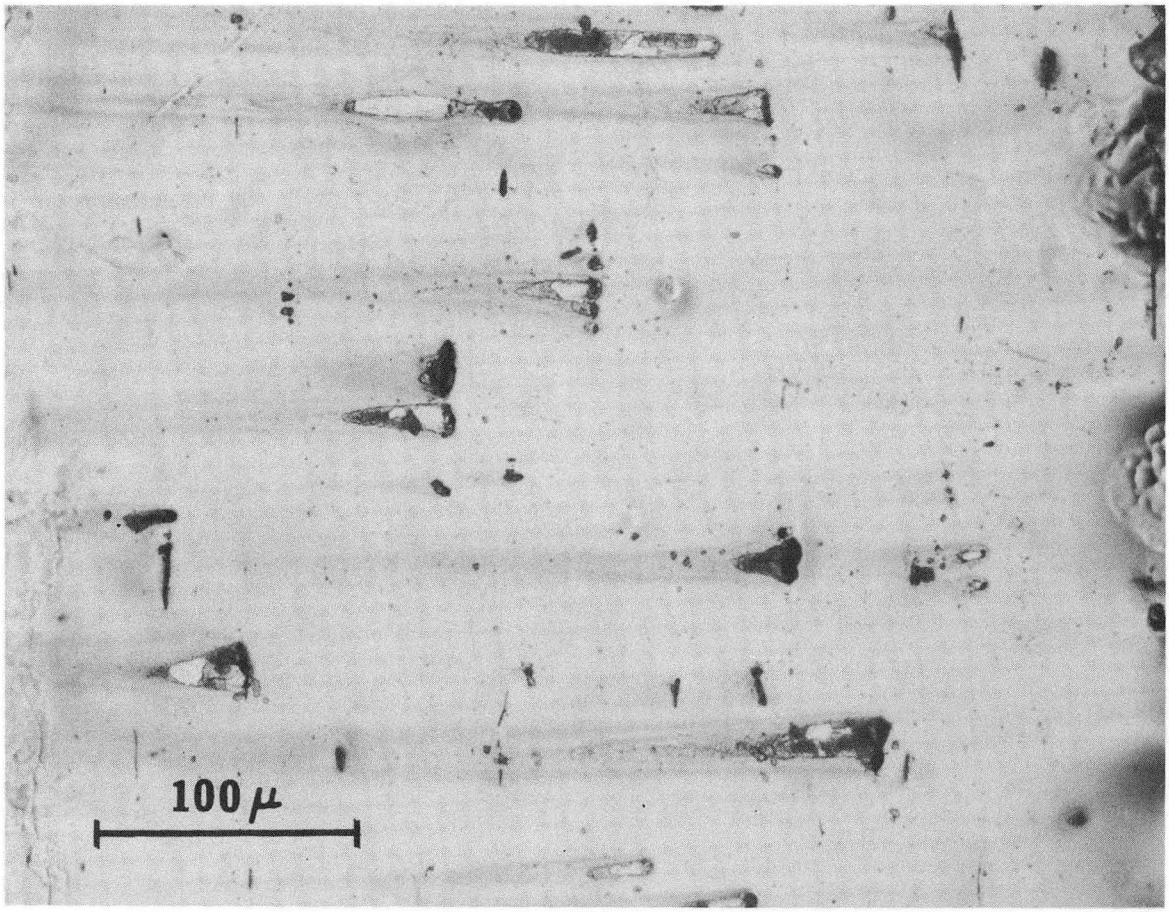

XBB 7111-5656

Fig. 15

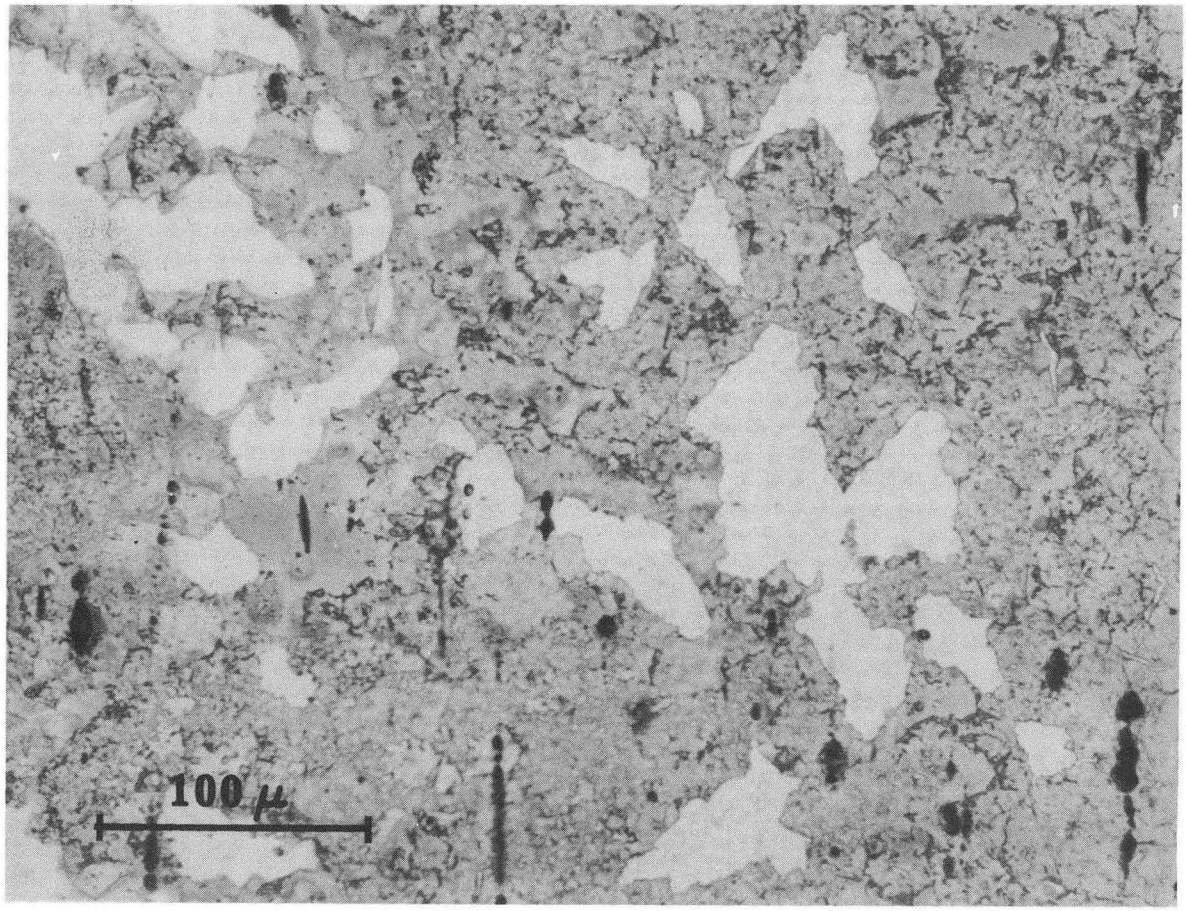

XBB 7111-5653

Fig. 16

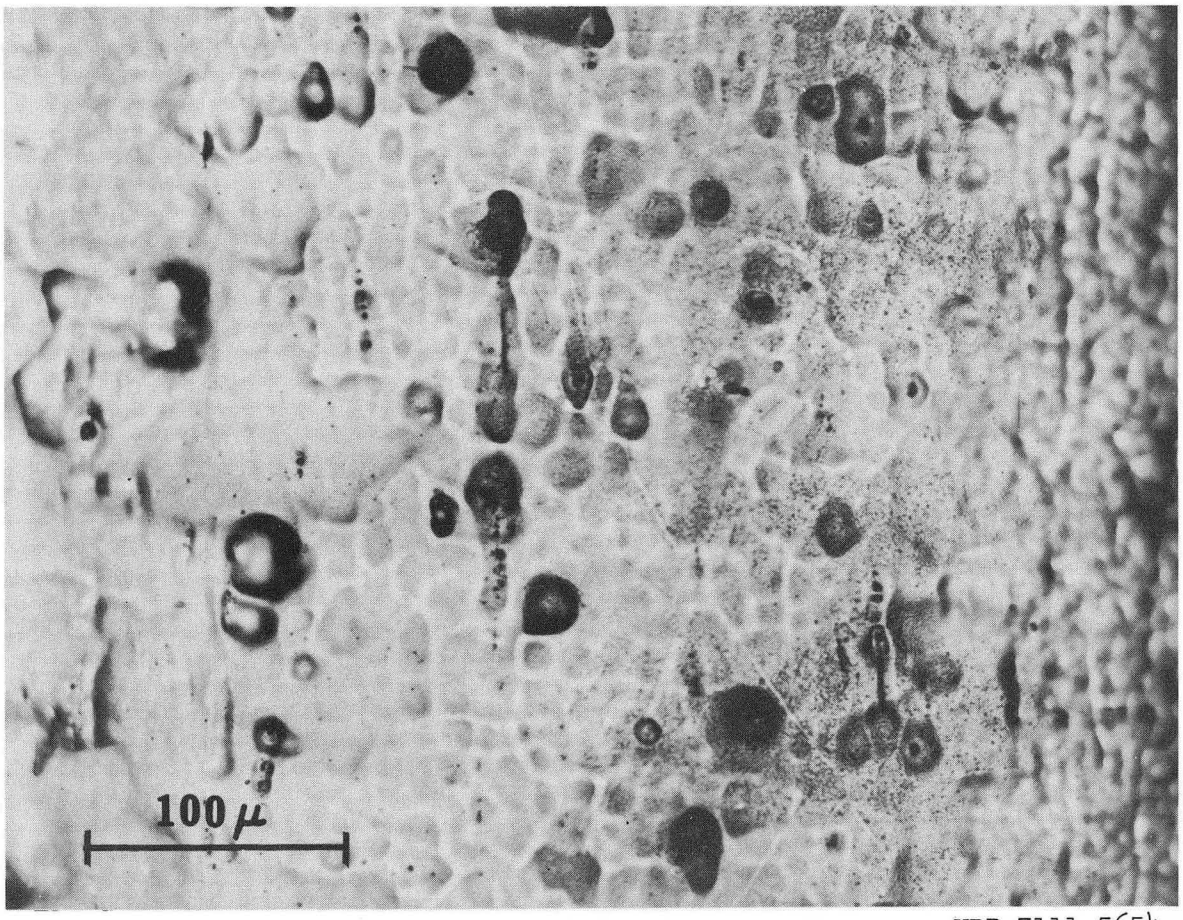

XBB 7111-5654

Fig. 17

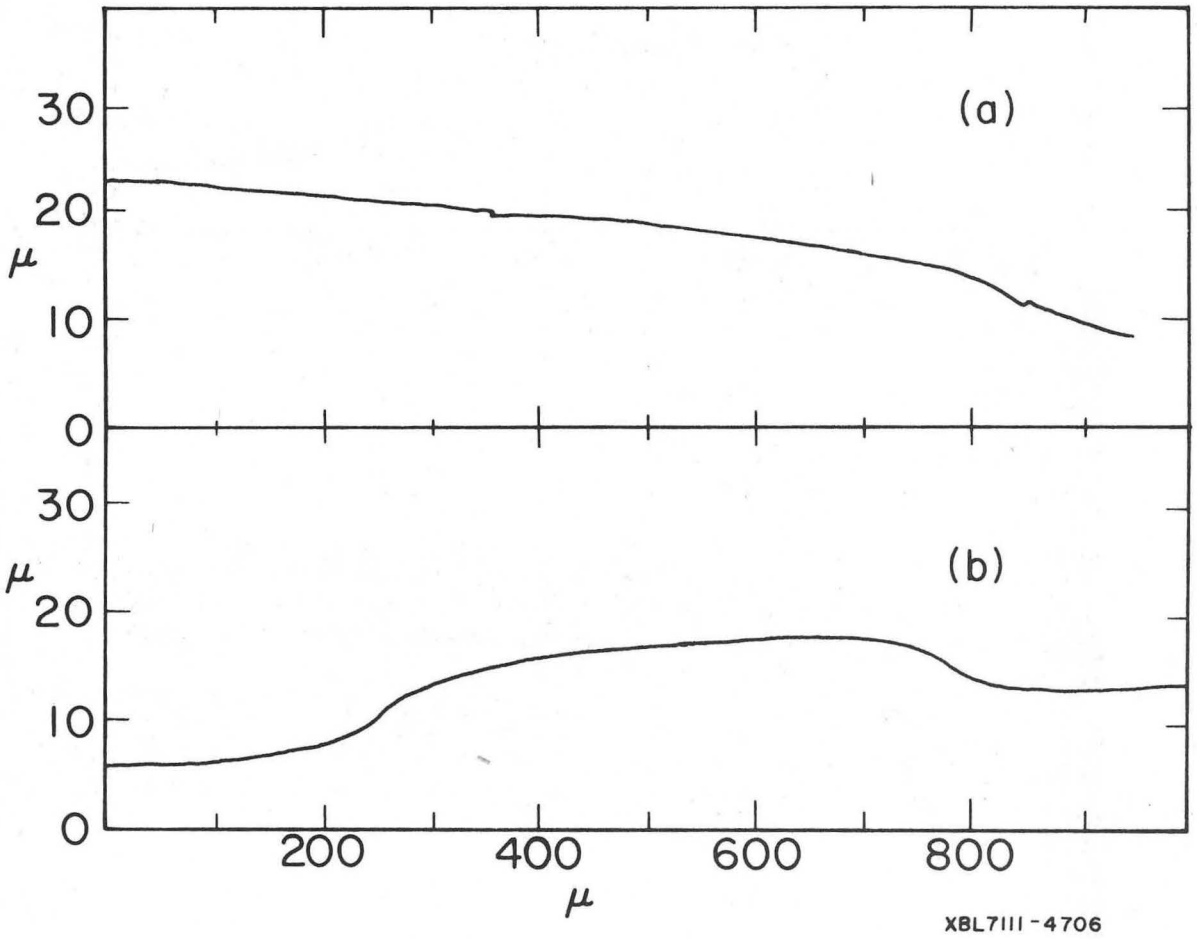

Fig. 18

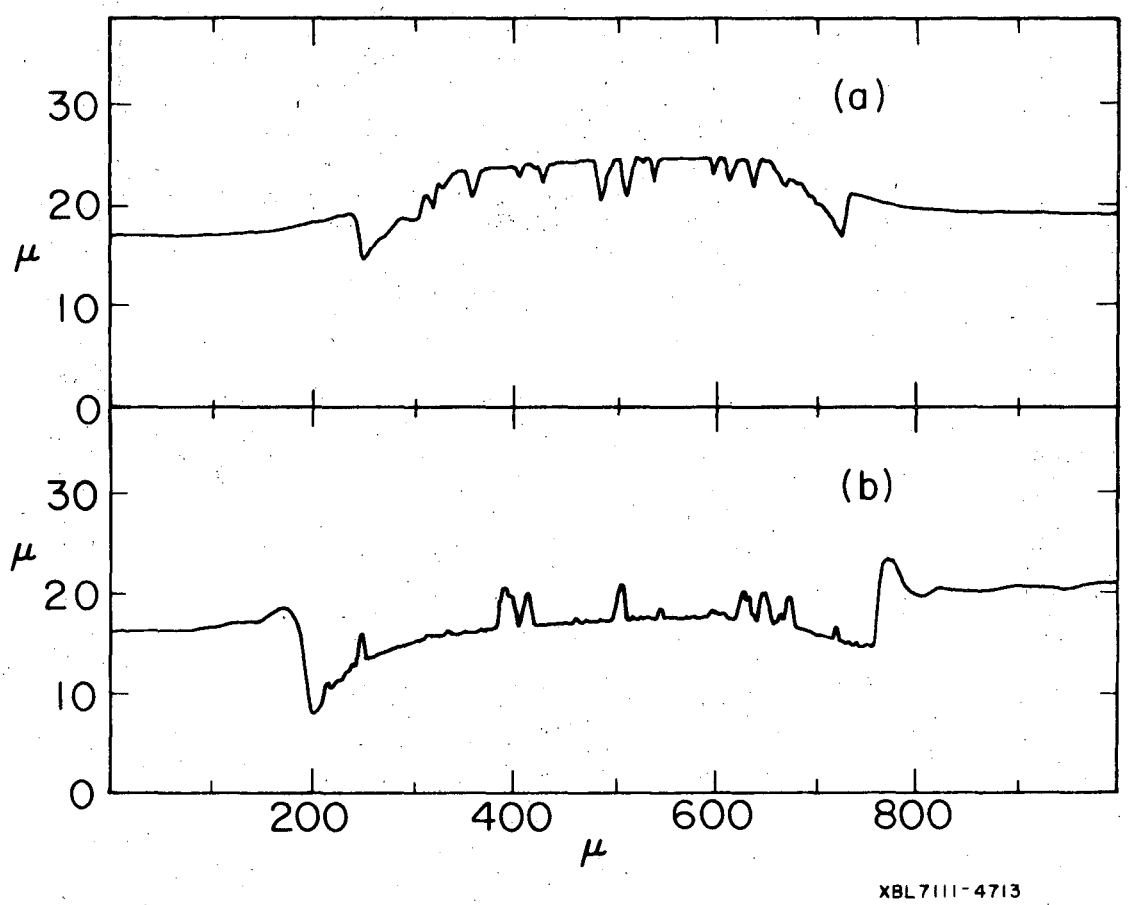

Fig. 19

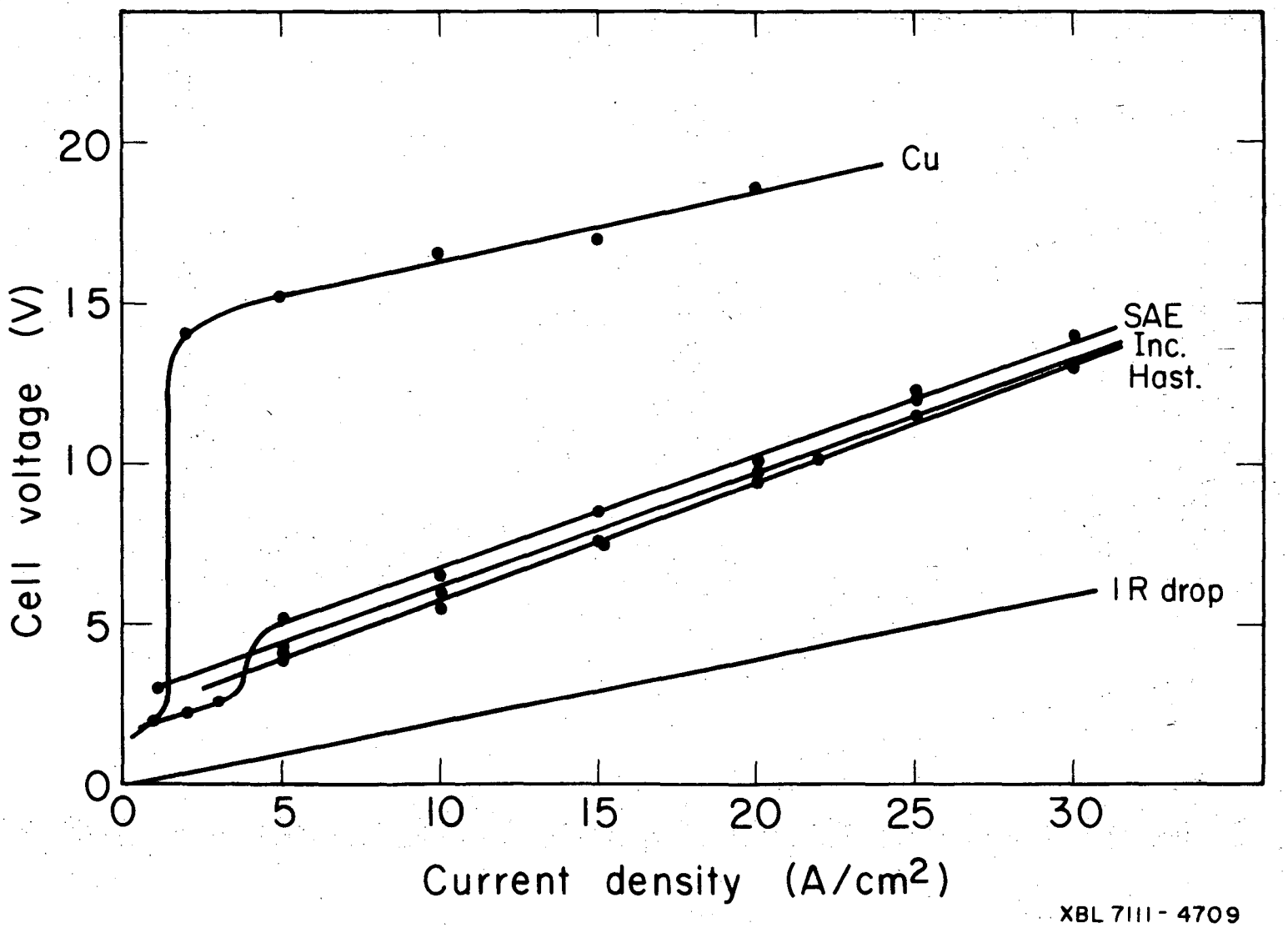
Cell voltage (V)
Current density (A/cm2)
0
5
10
15
20
25
30
Cu
SAE
Inc.
Hast.
IR drop
XBL 7111 - 4709

Fig. 20

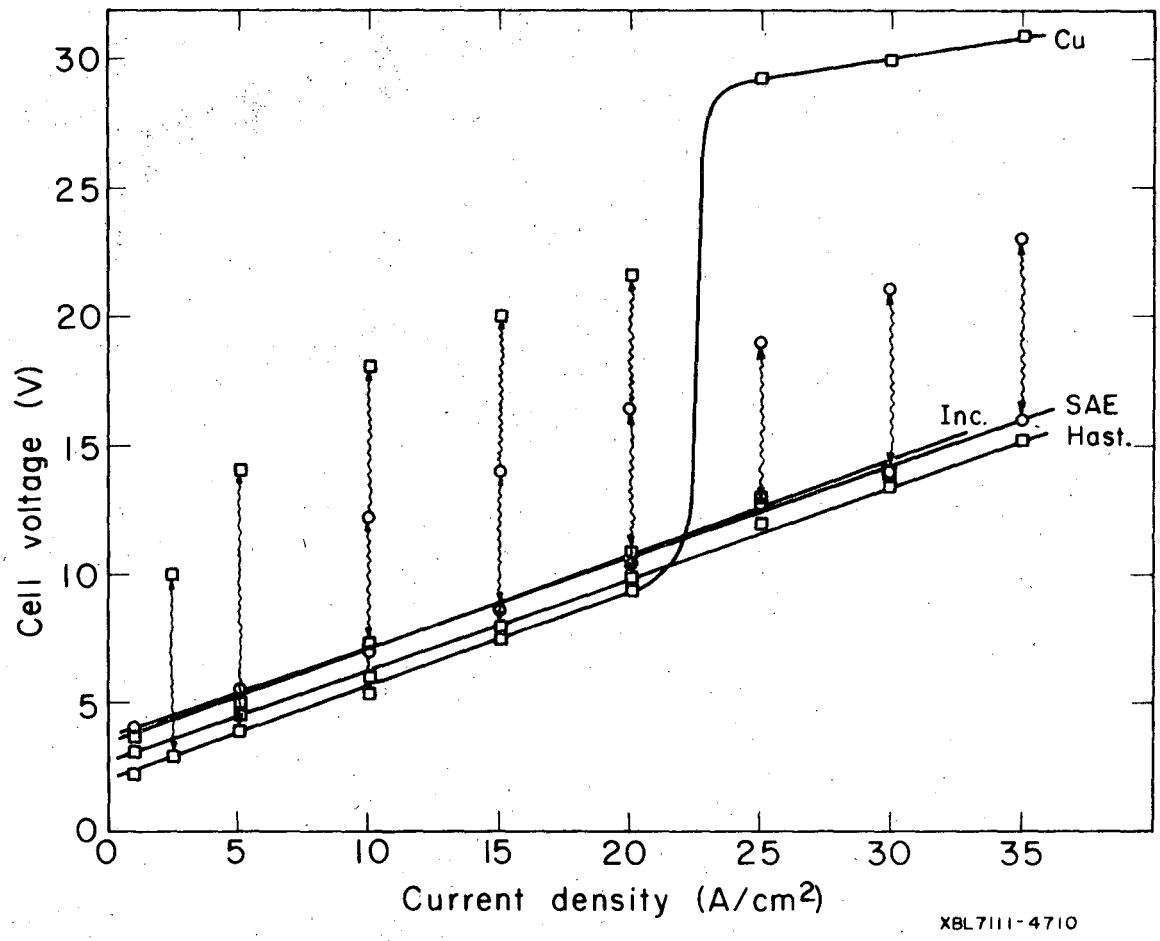
Cu
Inc.
SAE
Hast.
Cell voltage (V)
Current density (A/cm²)
0
5
10
15
20
25
30
35
XBL7111-4710

Fig. 21

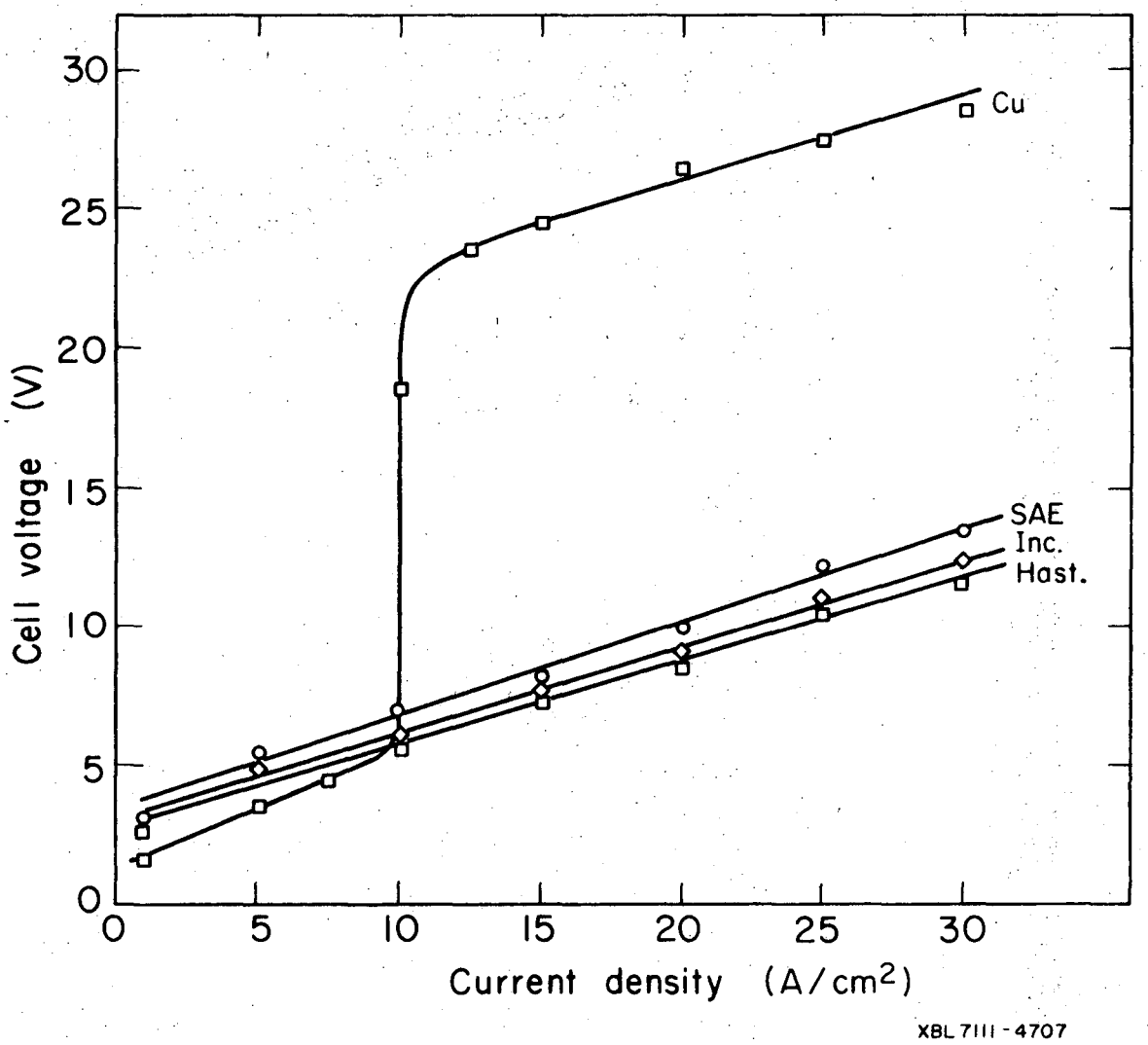
Cell voltage (V)
Current density (A/cm2)
Cu
SAE
Inc.
Hast.
0
5
10
15
20
25
30
XBL 7111-4707

Fig. 22

LEGAL NOTICE

This report was prepared as an account of work sponsored by the United States Government. Neither the United States nor the United States Atomic Energy Commission, nor any of their employees, nor any of their contractors, subcontractors, or their employees, makes any warranty, express or implied, or assumes any legal liability or responsibility for the accuracy, completeness or usefulness of any information, apparatus, product or process disclosed, or represents that its use would not infringe privately owned rights.

TECHNICAL INFORMATION DIVISION
LAWRENCE BERKELEY LABORATORY
UNIVERSITY OF CALIFORNIA
BERKELEY, CALIFORNIA 94720